SKB

TECHNICAL REPORT 91-45

The implications of soil acidification on a future HLNW repository. Part I: The effects of increased weathering, erosion and deforestation

Josefa Nebot, Jordi Bruno

MBT Tecnología Ambiental, Cerdanyola, Spain

July 1991

SVENSK KÄRNBRÄNSLEHANTERING AB
SWEDISH NUCLEAR FUEL AND WASTE MANAGEMENT CO

BOX 5864 S-102 48 STOCKHOLM

TEL 08-665 28 00 TELEX 13108 SKB S
TELEFAX 08-661 57 19

THE IMPLICATIONS OF SOIL ACIDIFICATION ON A FUTURE HLNW REPOSITORY. PART I: THE EFFECTS OF INCREASED WEATHERING, EROSION AND DEFORESTATION

Josefa Nebot, Jordi Bruno

MBT Tecnología Ambiental, Cerdanyola, Spain

July 1991

THE IMPLICATIONS OF SOIL ACIDIFICATION ON A FUTURE HLNW REPOSITORY

Part I: **The effects of increased weathering, erosion and deforestation.**

by Josefa Nebot and Jordi Bruno
MBT Tecnología Ambiental

TABLE OF CONTENTS

ABSTRACT

We have developed a model for soil acidification and granite weathering and erosion caused by the extended use of fossil fuels.

We have explored three different scenarios for depletion of fossil fuel reserves depending on how stringent is the control of the overall fossil fuel cycle.

Fossil fuels reserves are expected to last for the next 300 years. Nevertheless, we have extended our calculations up to next forecasted major glaciation period (58,000 years).

The results of the calculations can be summarized as follows:

- For the best and average scenarios the impact of soil acidification due to fossil fuel burning, lasts only for about 500 years. The overall effect is to increase the net surface lowering (weathering + erosion + denudation) in a few percentage (1-2%).

- In the worst case scenario, the impact of the fossil fuel combustion on the ecosystem is irreversible. The result being that up to 30% of the expected depth of the repository (500 m) would be eroded by year 60,000. The overall ecological impact of this scenario indicates that the safety of a HLNW repository would be a lesser problem for the Southern Sweden ecosystem.

1. INTRODUCTION

The Earth's global environment can be considered with regard to the mass transfer as an (almost) closed system. The atmosphere's outer layer, the stratosphere, acts as an interface between the system and the surroundings, allowing at the same time energy transfer.

The different compartments (atmosphere, geosphere and litosphere) forming our environment, the biosphere, can globally be considered to be in a steady state with respect to the redox reactions or to the proton and electron balances. Obviously, this global stationary state is locally and regionally disturbed. In fact, naturally occurring processes can cause the above-mentioned decoupling between proton producing and proton consuming reactions. One of this natural processes responsible for local proton imbalances is the aggradation of vegetation. In terrestrial ecosystems, accumulation of biomass occurs in inmature forests until the establishment of the definitive population of the stand.

In addition, other processes can cause the proton balance to be upset, i.e. the human activities. At the present moment, one of the major causes of these local and/or regional imbalances is the anthropogenic input of protons to the environment originating from the combustion of fossil fuels for energy.

The natural cycling of some principal elements, such as carbon, nitrogen and sulfur has been altered by the combustion of fossil fuels. This activity has caused the rate of the oxidation reactions to increase, while the reduction rates remain unaltered. Accordingly the concentration of oxidized compounds of the above mentioned elements has resulted globally increased in the case of CO_2, and locally or regionally increased in the case of sulfur and nitrogen oxides. This increase was first noticed in the troposphere due to the smaller volume and the relatively short mixing time of this reservoir.

Once in the atmosphere, sulfur and nitrogen oxides are transformed into the corresponding "strong acids", H_2SO_4 and HNO_3, which are quickly removed from the atmosphere and deposited in the litosphere.

Several processes in the soil, such as denitrification, sulphate reduction and chemical weathering can neutralize the human-enhanced deposition of acids. In the long-term, the quantitatively most important one is the chemical weathering of minerals. Carbonate minerals are widespread around the earth's crust. The carbonate rocks are easily weatherable minerals, exhibiting a fast kinetics of dissolution. Hence, they provide an enormous potential for neutralizing the acid load into the soil.

However, in some areas of North America and Fennoscandia, the dominant type of minerals forming the bedrock are crystalline rocks, such as granite, gneiss and quartz, which are only slowly weathered. In these regions, nor the shallow and base-poor soils deriving from the crystalline rocks neither the weathering of the bedrock itself, can keep pace with the acid deposition. This results in a transfer of this acidity to the downstream compartment in the acid flux: the hydrosphere. Within the hydrosphere, the subcompartment first showing the acidification effects is the surface water, namely lakes and streams. Groundwater can also be affected over long exposition to acid deposition. The element responsible for the acid flux to the surface waters is mainly aluminum, which has been exchanged into the soil solution by protons.

The first signs of local acidification were early noticed in areas where ore smelting was a current practice. Linné, in 1734, described that around a 500 years-old smelter at Falun (Sweden) no herbs could grow. However, the first major unification of knowledge about acid precipitation was achieved by Odén, a soil scientist of Uppsala (Sweden). In 1961, Odén's studies showed that acid precipitation is a large scale phenomenon and hypothesized that probable ecological consequences of the acid precipitation would be changes in surface water chemistry, decline of fish populations, leaching of toxic metals from soils, decreased forest growth and accelerated damage to materials. Unfortunately, at the present moment, Odén's hypothesis have been widely confirmed and this study itself is aimed at assessing the long-term consequences of the acid deposition on mineral weathering rates and soil erosion rates.

The objective of this report is to make a prospective study of the effects of the ongoing acidification of soils, surface waters and groundwater on the host rock of high level waste repositories in granitic formations. Two main impacts on the performance of such repositories can be expected:

1/ on the geological stability of the granitic formations through increased rates of chemical weathering and erosion and,

2/ on the chemical composition of groundwater.

This report will focus on the impact of acid deposition on the rates of weathering and erosion of granitic bedrock. The effects on the groundwater composition will be studied in a forthcoming report of this series.

Three different scenarios, based on the atmospheric emissions of CO_2 and SO_2, are explored up to next Ice Age, which is "scheduled" to happen in some 58.000 years (Ahlbom et al., 1990). A simple conceptual model is developed in order to asses the consequences of the environmental acidification for deep bedrock disposal.

Main attention is paid to deforestation as a consequence of acid deposition and to its role on increased rates of soil denudation.

2. SCENARIOS

The main cause of acid deposition is the release of SO_2 and NO_x into the atmosphere. The origin of the emissions of SO_2 is from natural sources, including both, geological activity (i.e. volcanoes and some hot springs) and biogenic activity. Anthropogenic emissions are mainly originated from the combustion of sulfur-containing fossil fuels. This is the quantitatively most important source of SO_2. More than 90% of SO_2 emissions in Eastern Europe and industrial areas of North America are the result of the burning of fossil fuels (Semb, 1978). The anthropogenic total emissions of SO_2 account approximately for 150 millions tons per year (Graedel, 1989). SO_2 emissions have nearly tripled in Europe since 1900, with the largest increase since the World War II (Semb, 1978).

NO_x released into the atmosphere is also originated from the combustion of fossil fuels and from the biomass burning. Some 40 millions tons of NO_x are yearly emitted into the atmosphere (Graedel, 1989).

Fossil fuels (coal, oil and gas) supply at the present 88% of global energy requirements and nuclear energy provides most of the rest (Gibbons, 1989). As fossil fuel combustion is the main source of SO_2 and NO_x, a central scenario related to this process is proposed. It is assumed the ratio of fossil fuel energetic supply to the nuclear one will be constant until depletion of fossil fuels, although this is very uncertain under present conditions.

Sulfur dioxide concentrations over Europe in last years were reviewed and projected 100 years ahead by Graedel et al.(1989) (Figure 2-1). These projections assume that population and energy consumption will grow and that the firing of coal for energy (a major source of SO_2) will increase.

Taking into account that the world coal reserves total about 950 billion metric cubic tons (Gibbons, 1989), at the today's production rates reserves will last for almost 300 years. Hence, in our calculations we have assumed that by the year 2300 the atmospheric acidity will peak.

Furthermore, three different sub-scenarios are studied depending on how stringent emission controls might be during next centuries: mild control (scenario A), moderate control (scenario B) or severe control (scenario C). These scenarios are based on the same criterium (SO_2 emissions) as in the RAINS model developed by the IIASA (Alcamo et al., 1990).

It is considered that the build-up of atmospheric SO_2 up to depletion of fossil fuels will continue at the rate estimated by Graedel et al. (1989) for next 100 years. A linear increase of varying slope is thought to be the most realistic approach to model the evolution of the atmospheric SO_2 concentrations (Figure 2-1), although from the mathematical point of view the best fitting for the measured and 100 years projected SO_2 concentrations is an exponential curve.

As a consequence, Eq 2-1, 2-2 and 2-3 are used to describe the build-up of atmospheric SO_2 (ppb) up to the depletion of fossil fuels.

$$SO_2A_{year} = 14 + 0.149*(year-1970) \quad \text{(Eq 2-1)}$$

$$SO_2B_{year} = 14 + 0.445*(year-1970) \quad \text{(Eq 2-2)}$$

$$SO_2C_{year} = 14 + 1.324*(year-1970) \quad \text{(Eq 2-3)}$$

Results of the calculations based on Eq 2-1, 2-2 and 2-3 for the expected sulfur dioxide concentrations in the atmosphere for the explored scenarios by the exhaustion of fossil fuels are shown in Table 2.1.

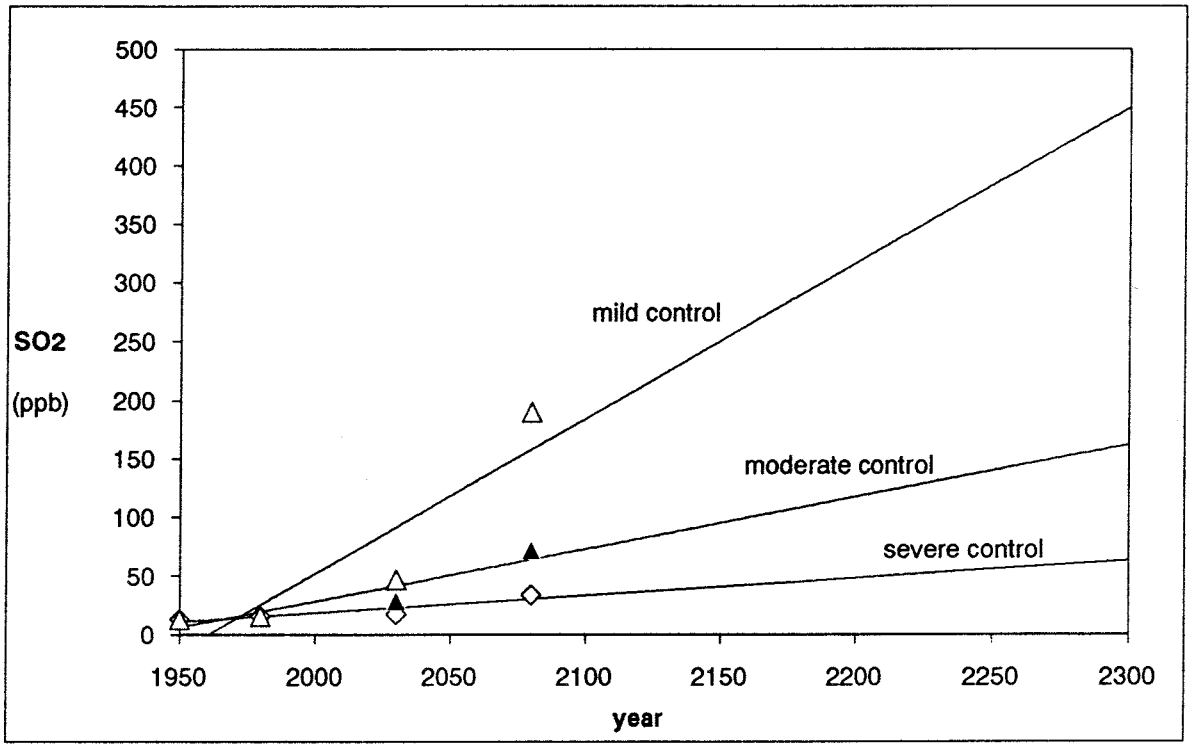

Figure 2-1. Measured and projected atmospheric concentrations of SO_2 (Graedel, 1989). The linear fitting of such data has been taken in order to model the evolution of atmospheric SO_2 concentrations up to the depletion of fossil fuels (2300).

It is well known that CO_2 concentration is also increasing in the atmosphere due to the same processes as SO_2 and NO_x (consumption of fossil fuels) as well as deforestation. This accounts for perhaps half of the build-up since the year 1800 and 20% of current emissions (Schneider, 1989).

The current average concentration is around 350 ppm, while the background concentration is estimated to be some 290 ppm (Raiswell 1983, Wayne 1985, Schneider 1989). The proposed scenario assumes a moderate increase of CO_2 during next centuries.

	CONTROL EMISSIONS	RATE OF INCREASE ($ppb.y^{-1}$)	$[SO_2]_{2300}$ (ppb)
scenario **A**	severe	0.149	63
scenario **B**	moderate	0.445	161
scenario **C**	mild	1.324	451

Table 2.1. Rate of increase and expected concentrations of atmospheric SO_2 over Europe at the depletion of fossil fuels (2300) depending on the explored scenario.

When making long-term predictions (more than 300 years) a moderate rate of increase of 0.8 ppm per year (Raiswell, 1983) is more realistic than the ones assumed in shortterm predictions i.e. 1.3 ppm per year as projected by Wayne (1985) or CO_2 concentration by 2000 to be 21% higher than the 1977 concentration (Sekihara, 1977).

Hence, we have studied in the various scenarios the increase in CO_2 concentration and consequently, the acidity and the buffering capacity of the CO_2-HCO_3^- system. The evolution of atmospheric concentration of CO_2 (ppm) from present to year 2300 is described by Eq 2-4.

$$CO_{2\ year} = 334 + 0.8*(year-1970) \qquad \text{(Eq 2-4)}$$

It has to be noticed that the evolution of the NO_x concentrations in the atmosphere is not considered in the scenarios. Two main reasons justify this assumption. The first one is the fact that reactions of oxidation of SO_2 in the atmosphere yield a sulfur residence time of several days; this corresponds to a transport distance of hundreds to a thousand kilometers. The formation of HNO_3 is more rapid, this results in a shorter travel distance, thus it can be assumed that nitrogen deposition accounts only for local acidification processes which are not considered in our regional model.

The second reason is that nitrogen is a growth-limiting nutrient in many terrestrial ecosystems in Europe and North America. Thus, a moderate additional input of nitrogen will usually lead to an increased primary production. A growing forest needs 0.5 to 0.8 $g.m^{-2}.y^{-1}$ of nitrogen.

This is partly confirmed by the fact that the analytical data from 12 Swedish stations performed by Rodhe et al. (1986) showed no further increase of NO_3^- in precipitation between 1972 and 1984.

The scenario developed considers that after depletion of fossil fuels (2300) the remainder of SO_2 is washed out from the atmosphere until its preindustrial level (background from natural sources).

The half-life of SO_2 in the atmosphere is assumed to be 10 days (0.027 years) and its natural background concentration 5 ppb. Assuming a first order kinetics, the removal of SO_2 from the atmosphere is described by Eq 2-5.

$$\ln SO_{2\ year} = \ln SO_{2\ 2300} - (25.3*(year-2300)) \qquad \text{(Eq 2-5)}$$

The CO_2 concentration in the atmosphere after depletion of fossil fuels will decrease slowly due to the fact that its average residence time in the atmosphere is estimated to be some 100 years. This is much longer than the average residence time of sulfur dioxide (a few days).

The decrease of atmospheric CO_2 is also considered to follow a first order kinetics, assuming 290 ppm as a final background pre-industrial concentration (this concentration corresponds to 1860 based upon data of Schneider, 1989) and a half-life time of 100 years, the decay of atmospheric CO_2 after depletion of fossil fuels is described by Eq 2-6.

$$\ln CO_{2\ year} = \ln CO_{2\ 2300} - (0.007*(year-2300)) \qquad \text{(Eq 2-6)}$$

Table 2.2 shows the half-life time and rate constants used to model the kinetics of removal of atmospheric SO_2 and CO_2 after depletion of fossil fuels.

Figure 2-2 depicts the decay of atmospheric CO_2 and SO_2 concentrations after exhaustion of fossil fuels.

After recovery of SO_2 and CO_2 background concentration, the scenarios developed are kept to cover a time span of some 58.000 years in which SO_2 and CO_2 levels remain constant until next Ice Age.

	HALF-LIFE TIME (year)	RATE CONSTANT ($year^{-1}$)	TIME REQUIRED RESTORE CONDITIONS (year)
SO_2	0.027	25.3	
scenario **A**			0.100
scenario **B**			0.137
scenario **C**			0.178
CO_2	100	0.007	106

Table 2.2. Half-life time, rate constants and computed time required to restore background concentrations of atmospheric SO_2 and CO_2 from 2300 (depletion of fossil fuels).

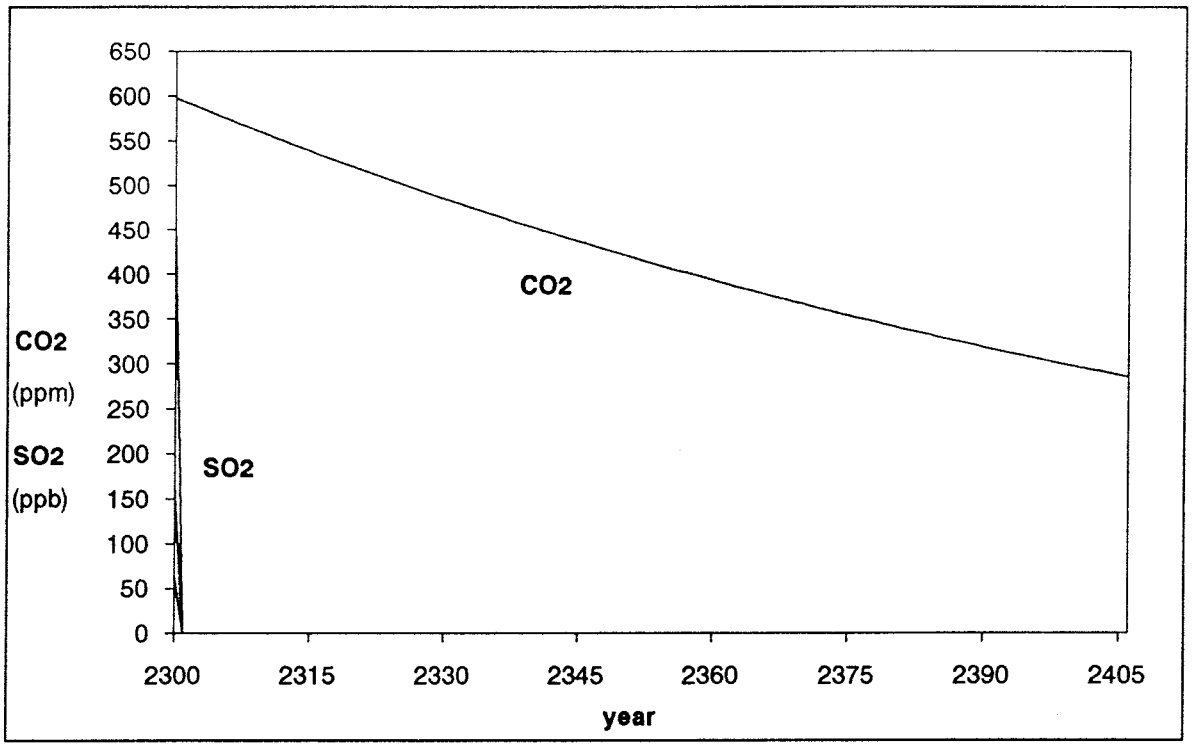

Figure 2-2. Decay of atmospheric CO_2 and SO_2 concentrations after depletion of fossil fuels.

3. DEFORESTING EFFECTS OF ACID PRECIPITATION

Although an increase in forest damage has been recorded in Europe and North America since the early seventies (Jacobson 1976, Johnson 1983), no consensus on its causes and mechanisms has yet emerged. Among the hypothesized causal agents are virtually all the pollutants species present in industrialized environments.

Our interest focuses on tree damage due to acid deposition, including both wet and dry deposition effects.

Basically, the suggested mechanisms of damage can be separated in two main groups:

- Direct effect of the gaseous pollutants on the foliage.
- Indirect effect on the root system through acidic deposition on soils.

The first mechanism is mainly exhibited by gaseous sulfur dioxide. In addition to adsorption on leaf surfaces, SO_2 enters the leaves through the open stomata and can cause abnormalities in cell structure and altered metabolic activity. In wet surfaces, SO_2 and dry deposited sulphate particles dissolve in water and the H_2SO_4 produced enhances the erosion of the leaf surface, which protect the leaf from the water losses and prevents leaching of nutrients from the foliage .

Furthermore, a mechanism of co-deposition of SO_2 and NH_3 in coniferous trees has been suggested (McLeod, 1990). This mechanism may cause an enhanced deposition of nitrogen compounds over large areas of Europe.

Acid deposition may cause soil changes detrimental to forest vegetation, either by stripping nutrients from the soils or by mobilizing phytotoxic elements.

It is still matter of discussion the way that acidic deposition on soils can cause the reported mortality of fine roots (Johnson, 1983) of declining trees. An increase of aluminum in soil solution was noted as was a calcium deficiency in roots in other declining stands. It has also been suggested that the ratio Al:Ca is responsible for the forest dieback (Wolt, 1990 and references therein).

It has been described that not only the SO_2 concentration, but also the period of exposure determines the degree of forest damage. For that reason the threshold concept can not be applied to tree damage caused by SO_2. The IUFRO Air Pollution Section, at this 1982 meeting in Oulu, Finland, decided that no safe limit could be set for SO_2 ambient concentration to protect forest trees (Tomlison, 1983).

In view of the variety of pathways to damage the trees as well as that there is no safe threshold, it seems quite reasonable to conclude that the effect of SO_2 on the forest trees is related to a physiological stress which makes the trees much more sensitive to other factors i.e. diseases and climate (Mäkelä, 1989).

The forest decline induced by acid deposition might eventually lead to a large areas of deforested land around Central and Northern Europe. The main consequences of such deforestation processes

concerning the geochemical stability of granitic formations are:

A/ Medium to poor forest soils are formed into podzols (the predominant soil type in Sweden). Podzolic soils exhibit a pronounced stratification. The litter accumulates on the top of the soil and it is slowly decomposed into humus by bacteria and mainly by fungi. The raw humus layer often exhibits a pH below 4. Some of the processes occurring in forested podzols concerning the acidic flux are:

- The regeneration of the cation store in humus layer is supplied by the decomposition of the litter. Tree roots act as a base cation pump through the A_2 and B horizons of the podzols (Jacks, 1984). The base cations originated by weathering in the B horizon are translocated in forested soils to the humus layer, by root uptake, litterfall and litter decomposition.

- Complex bacterial populations are supported in forested ecosystems, carrying out among others processes, the reduction of sulphate and denitrification. Both processes are a sink for hydrogen ions.

- The acid load into the soil due to nitrogen compounds is considered to be of lesser importance in front of sulphate deposition due to the uptake of such compounds during biomass growth (see 2. Scenarios). As deforestation proceeds, this sink of nitrogen compounds will disappear, thus, an increase in the acidity of the soil solution can be expected.

Hence, deforestation could result in a decrease of base saturation status in the top soil and in a decreased capacity of sinking protons and nitrogen compounds. This is likely to cause an increasing rate of acidification on such deforested soils.

It has been well established from laboratory studies that mineral weathering rates are dependent on hydrogen ion activity (Stumm and Wollast, 1990 and references therein). A field study conducted by Paces (1986) comparing two forested basins in Central Europe representing strongly acidified due to high deposition of SO_2 and less acidified environments of industrial and rural country-side, indicated increased weathering rates of bedrock and depletion of exchangeable cations from soils due to such an acidification.

Thus, from lab and field studies, it seems reasonable to conclude that an increase in proton activity in soils due i.e. to deforestation can account for a faster weathering rate.

B/ It is well known that afforestation is the best way to prevent soil denudation.

Denudation is a complex process involving detachment and downslope transport under the influence of both gravity (mass movement) and water in motion (slope erosion) (Slaymaker, 1988).

Weathering and soil formation are dependent upon several factors i.e. temperature, particle size, surface effects, biotic effects (White, 1990 and references therein) and variation in these factors causes the processes to proceed at different rates. If the rate of soil formation is defined as the rate at which rock is converted into soil, then weathering and soil formation are closely related processes, particularly in granite. On relatively pure limestone, however, a large depth of rock may weather giving only soluble species and leaving only a shallow soil.

Soil formation implies a loss of mass due to several processes i.e. dissolution of mobile elements. Although the bulk density of the soil formed is lower than the parent material bulk density (soil formation from bedrock implies an increase in the porosity), there is an overall reduction in the total volume of material, i.e. the volume of soil formed is less than the volume of rock weathered to form it. Hence, the process itself of bedrock weathering and soil formation implies a net surface lowering or landscape reduction, even without taking into account additional processes like denudation.

As an example, the rates of weathering and soil formation on granite were studied in two areas of Rhodesia using small watersheds (Owens 1979a, 1979b). The rate of granite weathering was calculated using Barth's equation (Barth, 1961) which links the rate of weathering to the amount of an element removed in solution per unit of time, its concentration on the rock and its concentration on the weathered product. Results of these field studies indicated rates of granite weathering of 15.4 and 11.0 mm per 1000 years for the higher and lower rainfall areas, respectively. The soil production rates were 11.0 and 4.1 mm per 1000 years. Thus, the net surface lowering rates were 4.4 and 1.7 mm per 1000 years, even in areas where soil production is high.

An estimation of the rate of surface lowering or landscape reduction under deforestation is a key point in this study. The maximum expected surface lowering rate corresponds to a situation where the soil is continuously removed while forming as it could happen in deforested areas. In this case, the rate of surface lowering is the same as the rate of bedrock weathering.

In southern Fennoscandia where thin soils are often found, deforestation could be responsible in short periods of time for total losses of existing soil due to denudation. In addition, no further recovery of soil mantle can be expected in deforested areas.

A deep mature soil over the bedrock protects it from weathering due to its buffer capacity. As the soil mantle thickens, the weathering zone is farther removed from the surface being decreased the available surface and consequently the weathering rate.

An example of the role played by the soil preventing the chemical weathering of the bedrock is the field study conducted in upland forested areas in New England (Hubbard Brook Forest). As mentioned by Johnson et al. (1972) only a moderate rate of weathering has been measured in this area in spite the acidification of their waters. The cause of this slow weathering rate is not clear. However, the maturity of the soil was suggested as a contributing agent.

On the other hand, in shallow or non-existing soils, fresh rock surfaces are constantly being created. These surfaces are completely exposed to physical, chemical and biological weathering agents.

Among the physical agents are precipitation and changes of temperature (freezing and melting processes) causing rock breakdown. Biological processes involve the direct colonization of bedrock by microflora and microfauna exerting a mechanical effect on rock as well as a chemical one releasing i.e. organic acids.

The final result of all these effects is again an increased rate of weathering of the bedrock.

The effects of deforestation discussed in **A** and **B** cannot be quantified separately. However, as it has been shown by Schnoor (1990) weathering rates measured in the field are always 1-2 orders of magnitude lower than the ones measured in the laboratory at the same pH conditions (Figure 3-1).

This has been rationalized by taking into account that the hydrological condition in the field is not the same as in the lab. Under ideal laboratory conditions, weathering proceeds much faster than in the field because of the larger availability of wetted surface.

A similar phenomena could be thought to be the final stage of deforestation, where maximum surface and porosity are available due to the disruption of the soil and "fresh" surfaces are continuously formed as a result of the increased erosion.

Hence, in our model the worst case scenario is considered to be the one causing total deforestation. This leads to a situation where weathering rates are large as the ones measured in laboratory studies.

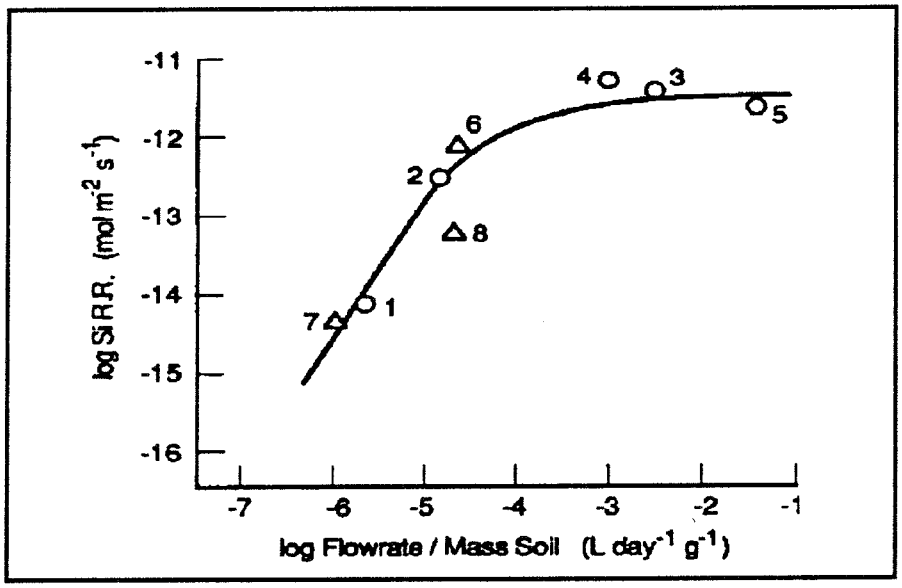

Figure 3-1. Dissolved silica release rate (weathering rate) versus flow-rate:mass ratio. (Schnoor, 1990).

4. DESCRIPTION OF THE MODEL

A conceptual model was designed to study the environmental acidification processes. The total sulfur concentration (as total sulphate) is considered the main driving variable of such processes.

A compartment structure (box model) was found to be a good approach to simulate the physically different reservoirs involved in the process of acidification. Such compartments or reservoirs are assumed to be connected by the transfer of sulfur compounds.

Four reservoirs were considered to be relevant in the natural flow of sulfur, namely atmosphere (troposphere), surface waters, soil-bedrock and groundwater. A schematic representation of the compartment system is shown in Figure 4-1. A more detailed description of the designed compartments and assumptions is given in next subchapters.

The model developed in this report refers to the atmosphere, soil and bedrock compartments. The modelling of surface and groundwater compartments is not considered in detail in this work. A regional model of the hydrological conditions of the region is under development. The consequences of the acidification processes in these compartments will be studied when a complete hydrological model for surface and groundwater mixing will be available.

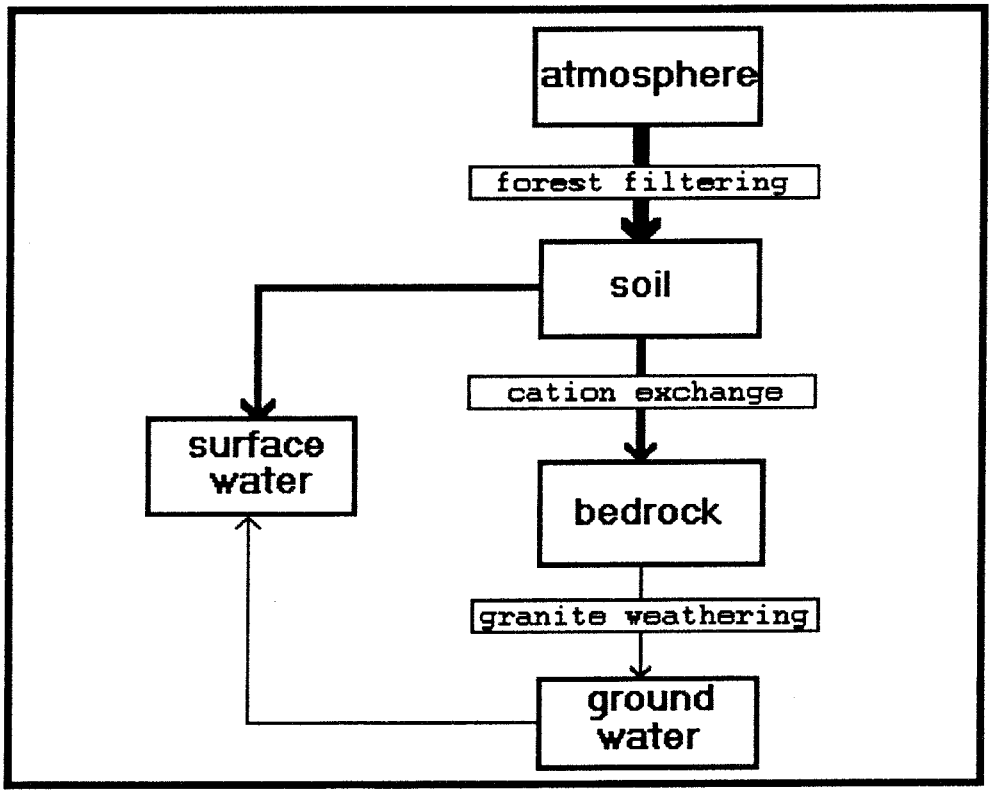

Figure 4-1. Schematic representation of the acid flux through the compartments involved in the developed model.

4.1. ATMOSPHERE

As mentioned above, the main driving variable for the environmental acidification processes is the total deposition of sulfur. In the developed model the atmospheric compartment is the origin of the acid flux, being sulphate the assumed species responsible for the acidic deposition.

Sulfur is emitted as a gas, sulfur dioxide, but it is transformed into fine sulphate particles once in the atmosphere (Bricard 1977, Wayne 1985). A process which, among others, gives sulphate particle is direct SO_2 photochemical oxidation, schematically shown as:

$$2SO_2 + O_2 + h\nu \text{ ---> } 2SO_3$$

where SO_3 is further hydrolyzed into H_2SO_4:

$$SO_3 + H_2O + M \text{ ---> } H_2SO_4 + M$$

The model assumes all the SO_2 is finally washed out from the troposphere in the form of H_2SO_4. No difference is considered in the deposition mechanism (dry or wet) on how the acidity reaches the soil reservoir.

The average SO_2 atmospheric concentration is used as the main variable in order to describe the scenarios. The sulphate concentration is considered to drive the acidification of soils. Hence, a linkage between SO_2 atmospheric concentrations and sulphate deposition has to be defined.

A direct correlation is assumed between SO_2 atmospheric values and sulphate concentration in precipitation on Southern Sweden. In order to obtain an average value for sulphate concentration in rainwater in this area, we relied on data taken from the European Air Chemistry Network.

The area considered comprises from 55ºN to 60ºN latitude and from 10ºE to 20ºE longitude (basically, Central and Southern Sweden). Around this region 44 stations were monitored for rainwater chemical data between 1955 and 1979 by the Swedish University of Agricultural Sciences of Uppsala and the International Meteorological Institute of Stockholm (Rodhe, 1984a). We used selected data sets (see Appendix A) to calculate the average sulphate concentration in rainwater in 1970.

Median values of each station have been used to estimate average sulphate concentration in precipitation in the concerned area as suggested by Rodhe et al. (1984a,b). The calculated value was assigned to 1970 as the origin of our calculations.

The available sulphate values (Rodhe, 1984a) referred to excess sulphate (i.e. the non-seasalt fraction). Since in ocean islands and coastal areas sulphate originating from seaspray contributes very significantly to the sulphate concentration in precipitation samples, the seasalt fraction of sulphate was deducted by Rodhe et al. based on the sodium concentration according to the following formula:

$$[SO_4^{2-}]_{ex} = [SO_4^{2-}] - 0.25\,[Na^+]$$

In order to calculate the total sulphate concentration (seasalt + non-seasalt), the sodium average concentration in precipitation has to be known. This value was calculated from the data of the sodium contain in precipitation taken from Söderlund et al. (1981) by using median values of each station. The average sodium content in precipitation was calculated to be 47 $\mu mole.dm^{-3}$.

The computed average excess sulphate content of the rainfall was 47 $\mu mole.dm^{-3}$. Hence, the calculated total concentration of sulphate was 58 $\mu mole.dm^{-3}$. This concentration was taken as a base level corresponding to 1970 for next calculations.

All calculations were made by taking as average for the region considered an annual precipitation of 1000 $mm.m^{-2}$ (Tanke, 1989 and references therein).

The linear relationship between time and concentration of sulphate ($mole.dm^{-3}$) in precipitation is described for each scenario by Eq 4-1, 4-2 and 4-3.

$$SO_4^{2-}A_{year} = 5.8*10^{-5} + 0.497*10^{-6}*(year-1970) \quad \text{(Eq 4-1)}$$

$$SO_4^{2-}B_{year} = 5.8*10^{-5} + 1.403*10^{-6}*(year-1970) \quad \text{(Eq 4-2)}$$

$$SO_4^{2-}C_{year} = 5.8*10^{-5} + 5.067*10^{-6}*(year-1970) \quad \text{(Eq 4-3)}$$

In order to validate the reliability of such equations to predict the total sulphate concentrations of the rainfall, a check against the measured concentrations during the eighties was made.

Our results are in good agreement with the measured data of the Co-operative Program for the Monitoring and Evaluation of the Long Range Transmission of Air Pollutants in Europe (EMEP) (in Hordijk et al. 1989). These data are presented as isolines of volume-weighted average of sulphate in precipitation on Europe (1978-1982). Southern Scandinavia falls between the 1.5 and 4.5 mg SO_4^{2-}-$S.dm^{-3}$ isolines. Assuming the scenario B (moderate control of emissions), the one actually operating in Scandinavia, we estimate a sulphate concentration of 2.3 mg SO_4^{2-}-$S.dm^{-3}$.

Base cations can neutralize in the atmosphere a substantial amount of acid deposition, this has to be considered in order to calculate the acid load entering the soil compartment.

Alkalies are generated in the atmosphere as the carbonates of wind-blown dust, generally of natural origin, and from seaspray in coastal areas. It is known from precipitation measurements (Likens, 1979) that most of the base cation contain is in the form of calcium and magnesium.

It is difficult to quantify base cation deposition. As noticed by Kämari (in Kauppi et al., 1989) the ratio base deposition/sulfur deposition is fairly constant. The combined Ca^{2+} and Mg^{2+} deposition was estimated to neutralize an average of 33% of the sulfuric acid in bulk precipitation, within a range of 12% to 44%. Hence, we assume in the model that one third of the sulfuric acid is readily neutralized in the atmosphere before reaching the soil.

The computed total acidity (Htot) of rainwater as a function of SO_4^{2-} concentration and dissolved CO_2 ($H_2CO_3(aq)$) in mole.dm^{-3} for each scenario is described by Eq 4-4.

$$HtotA,B,C_{year} = 1.33*SO_4^{2-}A,B,C_{year} + 2*H_2CO_3(aq)_{year} \quad \text{(Eq 4-4)}$$

where $H_2CO_3(aq)_{year}$ is calculated from CO_2 Henry's constant as shown below in Eq 4-5.

$$H_2CO_3(aq)_{year} = 1.132*10^{-5} + 2.711*10^{-8}*(year-1970) \quad \text{(Eq 4-5)}$$

Due to the composition of rainwater, the total and free acidities are almost similar and H^+ concentration approximates the Htot (Johnson, 1985). The expected pH values of the rain solution in southern Sweden are shown for the three studied scenarios in the period 1970-2300 in Figure 4-2 below.

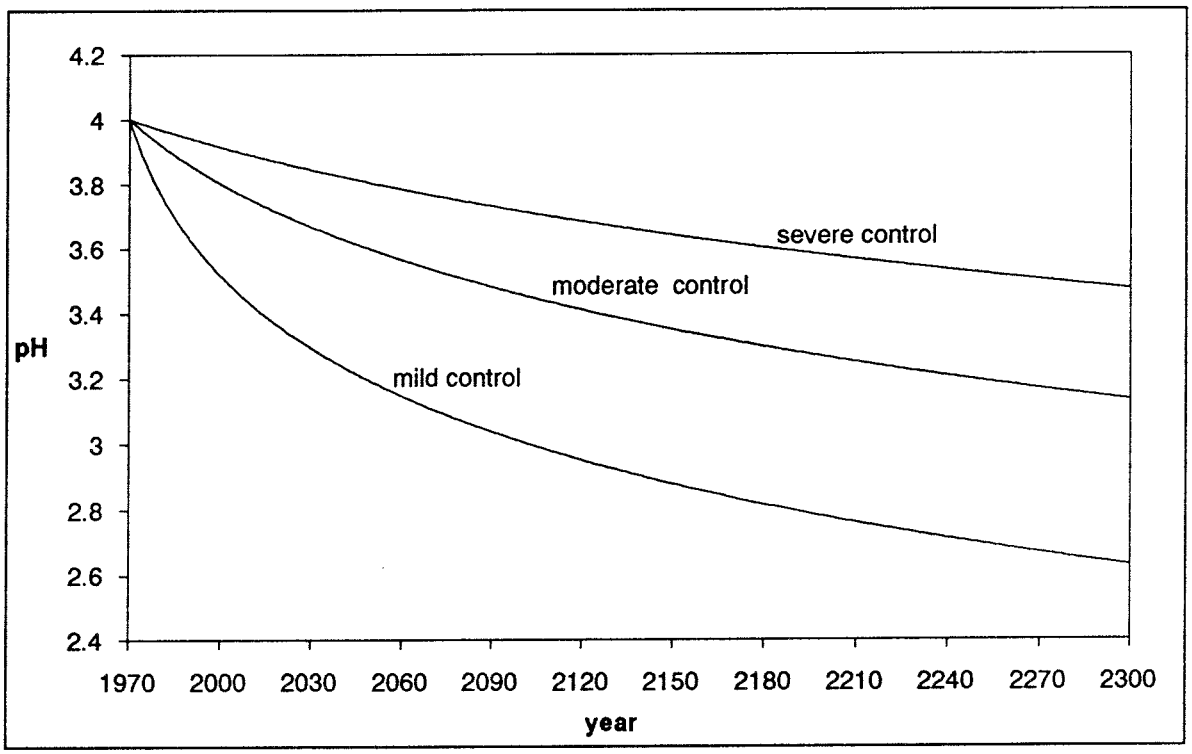

Figure 4-2. Evolution of the rainwater pH depending on the scenario explored up to depletion of fossil fuels (1970-2300).

4.2 SOIL-BEDROCK

The soil is considered in this model as an interface between the atmosphere and the bedrock, for this reason they are not treated as a separate reservoirs.

This chapter is devoted to the acidification processes which occur in forested soils. Since agricultural soils are intensively managed with lime and other chemicals, acidification is not expected to proceed in these soils. Furthermore, one of the objectives of this study is to assess the degree of deforestation due to acid deposition.

4.2.1.Processes of acidification in forested soils

Van Breemen et al. (1984) defined soil acidification as a decrease in the soil acid neutralizing capacity (alkalinity) accomplished by removal of alkaline earth cationic components or, to a lesser extent, by addition of acidic components.

Soil acidification occurs by an irreversible flux of protons to the soil. Proton sources include:

- atmospheric inputs of acidic or potentially acidic substances
- net assimilation of cations by vegetation
- net mineralization of anions from organic matter
- deprotonation of weak acids
- oxidation reactions
- precipitation of cations as a consequence of secondary phase formation
- mineral weathering of anionic components

We will only consider the first point which represents the anthropogenic input of protons to the soil system (acid deposition), whilst the rest are taken as background processes which do not upset the global balances.

Protons entering or produced in the soil are removed by:

- export in drainage water
- net mineralization of cations in organic matter
- net assimilation of anions by vegetation
- protonation of anions
- reduction reactions
- weathering of cationic components
- precipitation of anions

Once the acid input to the soil is completely neutralized, cations are removed by vegetation uptake and/or export into drainage water, resulting in soil acidification and in an increase in the alkalinity of percolating water.

Different reactions are responsible for the buffer capacity of the soil. The concept of buffer capacity corresponds to the above mentioned concept of alkalinity or acid neutralizing capacity used by Van Breemen and can be defined as the total reservoir of basic components in the soil.

Ulrich (1981, 1983) (in Berdén et al., 1987) classified the inorganic buffering reactions in the following buffer ranges:

- **Carbonate buffer range**: the buffering capacity in this range is supplied by $CaCO_3$ (Eq 4-6), hence only calcareous soils are within this range. The amount and the rate of dissolution of $CaCO_3$ in such soils is usually enough to buffer moderately large amounts of acidic deposition. The pH of the soil solution within this range is higher than 6.2.

$$CaCO_3 + H^+ = HCO_3^- + Ca^{2+} \qquad \text{(Eq 4-6)}$$

- **Silicate buffer range**: this corresponds to the buffering range of feldspar weathering reactions which can be generalized as described by Eq 4-7.

$$KAlSi_3O_8 + 7\ H_2O + H^+ \text{ ---> } Al(OH)_3(s) + 3\ H_4SiO_4 + K^+ \qquad \text{(Eq 4-7)}$$

These are kinetically slow reactions and cannot be described as an equilibrium buffer capacity. Hence a silicate buffering rate capacity is defined. This corresponds to the rate of reaction 4-7. The pH of the soil solution in this range is between 5.0 and 6.2.

- **Cation exchange buffer range**: base cations such as Ca^{2+}, Mg^{2+}, Na^+ and K^+ exist in the soil mainly complexed by the organic matter (humic and fulvic substances) and/or bound to clay particles.

The buffer capacity given by exchange reactions with humic substances can be described by a general reaction (eq 4-8) as follows:

$$HUM\text{-}Ca + 2\ H^+ = HUM\text{-}H_2 + Ca^{2+} \qquad \text{(Eq 4-8)}$$

The buffer capacity given by surface reactions on clay particles may be generalized in reactions of the type:

$$>SiOK + H^+ = >SiOH + K^+ \qquad \text{(Eq 4-9)}$$

where the symbol > denotes a surface process.

These two processes are kinetically fast and they constitute the more readily available buffering capacity of non-calcareous soils.

The number of reactive sites available is approximated to the Cation Exchange Capacity (CEC). Base saturation (ß) is the fraction of CEC consisting in base cations. Buffer capacity of the cation exchange range (ßCE) is defined as the product of CEC and ß.

If the total acid load overalls the cation exchange buffer capacity, this buffer becomes depleted and silicate weathering becomes the only neutralizing process available. The pH of the soil in this buffer range is between 5.0 and 4.2.

- **Aluminum hydroxide buffer range**: as the alkalinity of the soil solution is depleted and as a consequence of feldspar weathering, Al(III) hydroxide becomes abundant in the soil solution. At the low Al(III) concentrations and pH range of this buffer (pH= 4.2 to 3.0), the main equilibrium is given by :

$$Al(OH)_3(s) + 3\ H^+ = Al^{3+} + 3\ H_2O \qquad \text{(Eq 4-10)}$$

For poorly crystallized gibbsite this is a fast reaction.

If this buffer capacity is exhausted, other solid phases dissolution and precipitation reactions can take over. For instance, $Fe(OH)_3(s)$ dissolution has been considered to buffer the soil solution at very low pH values.

4.2.2 Main assumptions of the model developed

In our effort to model the process of soil acidification in Southern Fennoscandia, we assume, based on data taken from the FAO-UNESCO Soil Map of the World (1974) (in Kauppi et al. 1989), that the type of forest soil predominant in the area to be studied is orthic podzol. The orthic podzol is a non-calcareous soil deriving from granitic or base-poor material.

Podzols in Scandinavia are often shallow soils, exhibiting a pronounced stratification. On the top of the soil it is found a humus layer originating from the slow decomposition of litter. The pH of this layer is often below 4 in medium to poor podzols. A bleached horizon (A_2), usually grayish in color due to intense leaching, follows below the raw humus layer. Below this layer, there is an enrichment zone, the B-horizon, reddish to brownish. Iron leached from the bleached horizon precipitates here in trivalent form as goethite (Jacks, 1984).

In order to simplify the calculations, the model assumes that the soil layer is a homogeneous box 50 cm deep. In addition, we deal with yearly variations in soil acidification in order to avoid seasonal fluctuations. This seasonal variations are mainly caused by biological activity and tend to be internally compensated in the ecosystem over the year.

Since podzols are non-calcareous soils, it is postulated that the carbonate buffer range has been surpassed. Therefore, the model assumes that at the origin of our calculations (1970) the soils considered here are at the stage at which cation exchange is the dominant buffer reaction.

Cation exchange buffer capacity (ßCE) includes in our model the ion exchange capacity of the organic substances as well as the cation exchange from silicate interlayer positions by a slow diffusion phenomenum reported in young soils of Scandinavia by Graunstein (1981) (in Jacks et al., 1984).

It is postulated that the soil exhibits some capacity of recovery in front of acid deposition due to the organic matter, represented in our model by an initial term (ßCE0). This recovering capacity is assumed to be linearly depleted with time at the same rate as acid load increases as computed in Eq 4-11, 4-12 and 4-13.

$$\beta CE0A_{year} = 2.0 - (7.182*10^{-4}*(year-1970)) \quad \text{(Eq 4-11)}$$

$$\beta CE0B_{year} = 2.0 - (1.924*10^{-3}*(year-1970)) \quad \text{(Eq 4-12)}$$

$$\beta CE0C_{year} = 2.0 - (6.809*10^{-3}*(year-1970)) \quad \text{(Eq 4-13)}$$

Silicate weathering rate (see section 4.2.4) is assumed to be only slightly dependent on the soil solution pH. If we assume that the weathering rate (brSi) is proportional to $[H^+]^{0.5}$, a decrease of pH in the soil solution of 2 units results in a ten-fold increase in the rate of weathering. In addition, the rate of release of base cations is assumed not to depend on the soil pH.

The modifying effect of the forest canopy (forest filtering) on the deposition is also taken into account in the model. There are two ways in which the canopy is modifying precipitation input to soil. One way is dry deposition. From an ecological point of view, any vegetation canopy behaves like a filter or a sink for the fluxes of matter passing along its surface, the filter efficiency being very dependent upon its physical and chemical properties (Mayer et al., 1978). Hence, forest filtering can cause forested soils to receive more sulfur deposition than adjacent cropland or pastureland.

Another way of modifying soil input is by leaching substances previously taken up by the roots and translocated to the upper parts of the tree. Thus, when they get to the soil surface the total precipitation input to soil is a mixture of substances coming from outside the ecosystem, i.e from the atmosphere, and other compounds which are merely completing an internal cycling (Mayer et al., 1978).

In addition, it has been shown by Ivens (1988) (in Kauppi et al. 1989) that forest filtering is quantitatively different in coniferous stands or in deciduous stands. The total surface of the needles of coniferous trees is bigger than the total surface of broad-leaved trees. Furthermore, in wintertime deciduous trees loose their leaves, while coniferous needles are kept through the year. Both factors cause the coniferous stands to intercept much more acid deposition than the deciduous stands.

It is difficult to quantify the concentrating effect of coniferous canopies. Our model assumes that soil under coniferous trees receives an acid load due to sulfur compounds 1.6 times greater that soil under deciduous trees as suggested by Kauppi et al. (1989).

In our model the net surface lowering is defined as the depth of bedrock weathered minus the depth of soil subsequently formed. A direct correlation between the assumed silicate weathering rate and bedrock surface lowering rate is assumed in order to calculate the net surface lowering.

One of the critical assumptions of the model is that once acidification proceeds further to the $Al(OH)_3$ buffer range, deforestation proceeds for the lifetime of the forest stand (50 years). Deforestation causes the total lost of soil mantle due to the increased effects of erosion and denudation. In these conditions the dissapearence of the soil mantle is irreversible and there is no longer soil formation.

As a consequence, due to the disruption of the soil structure, the bedrock surface becomes more available and the weathering rates get closer to the ones measured in ideal laboratory conditions.

4.2.3 Assignment of values to soil parameters

A key point in the development of any regional model is the correct quantification of the parameters involved in the model such as, in our case, cation exchange capacity and base saturation.

Ideally, field measurements of the relevant soil parameters should be preliminary to modelling and forecasting. In our study, since direct field measurements of such soil parameters were not accessible, literature values had to be relied upon. Following an extensive literature search it was decided to use the data elaborated by Kauppi et al.(1989) based on data reported in the Appendix of the FAO-UNESCO Soil Map of the World (1974).

In our model, initial conditions (1970) are always set to the less favorable conditions. The CEC and ß values are initially set to 20 moles.m^{-2} and 0.1 respectively, giving a cation exchange buffer capacity of 2.0 moles.m^{-2}.

Silicate weathering rates were also taken from Kauppi et al. (1989) (and references therein). These weathering rates were calculated from the data reported in the Geological Map of Europe and the Mediterranean Region. The initially assigned silicate weathering rate is 0.05 mole.$m^{-2}.y^{-1}$. The weathering rates measured across Europe range from 0.02 to 0.2 mole.$m^{-2}.y^{-1}$ (Ulrich, 1983 in Kauppi et al., 1989).

It is postulated that if the pH of the soil solution drops into the $Al(OH)_3$ range, the silicate weathering rate increases 1.5 orders of magnitude as a consequence of the disruption of the soil and larger availability of wetted surface. The assumed increase is based on the discussion given in section 3.

We assume that the above mentioned effect of soil disruption caused by extensive acidification over the $Al(OH)_3$ buffer range, increases 1.5 orders of magnitude the silicate weathering rates. This is based on the observations and discussions of section 3 regarding the differences between measured weathering rates in laboratory and field conditions. Under these conditions, the silicate weathering rate ($brSi_{Al}$) is assumed to be 1.58 moles.$m^{-2}.y^{-1}$.

Lerman (1988) reported rates of bedrock surface lowering, elaborated from chemical weathering field measurements conducted by Wright (1988) in different geological environments, ranging from 0.006 to 0.14 mm.y^{-1}. An intermediate bedrock lowering rate of 0.075 mm.y^{-1} is used in our model. The assumed rate of soil formation from granite is 9.10^{-3} mm.y^{-1} (Slaymaker, 1988).

A conversion coefficient (f) of $1.5*10^{-3}$ is used in our model to relate silicate weathering rate (mole.$m^{-2}.y^{-1}$) and bedrock surface lowering rate (m.y^{-1}) based upon the assigned values to bedrock surface lowering and chemical weathering rates.

A list of the symbols used along this chapter and its correspondence with the ones used in the RAINS model is given in Appendix B.

4.2.4 Model development

The main features of the developed model can be summarized as follows:

- calculation of the annual acid load entering the soil
- determination of the dominant buffering range
- calculation of the annual soil pH
- calculation of the net surface lowering at the corresponding year

The model computations are separated into the following steps:

1. The acid load entering the soil per year (HA,B,C_{year}) is calculated from total acidity of rainwater (Eq 4-4) assuming an annual precipitation of 1000 mm. m^{-2}.

2. The annual cation exchange buffer capacity (βCE_{year}) is calculated by subtracting the silicate weathering rate (brSi) from the acid input into the soil. This result is then subtracted from the annual initial buffer capacity of the cation exchange range ($\beta CE0$). These calculations can be represented as:

$$\beta CE_{year} = \beta CE0_{year} - (H_{year} - brSi) \qquad \text{(Eq 4-14)}$$

This is an annual iterative step while soil $\beta CE>0$ (the cation exchange buffer capacity of the soil is enough to neutralize the annual acid load). If $\beta CE=0$, it is considered that the soil drops into the $Al(OH)_3$ buffer range.

3. The soil pH is calculated within the silicate, cation exchange and upper aluminum buffering ranges ($\beta>0$) according to a non-linear relationship between base saturation and pH developed by Reuss (1983), as follows:

$$pH_{year} = 4.0 + 1.6 * (\beta CE_{year}/CEC)^{0.75} \qquad \text{(Eq 4-15)}$$

4. The silicate weathering rate ($brSi_{year}$) is recalculated as a function of pH in periods where acid load entering the soil is high (1970-2300). The weathering rate constant (k_{Si}) is calculated assuming a 0.5 order dependence on free proton activity.

5. The total amount of silicate weathered (WSi) during any period is calculated by integrating the weathering rate equations within that period.

6. The net surface lowering (NSLow) is calculated by establishing a direct correlation between the amount of silicate weathered (WSi) during the corresponding period, the bedrock surface lowering rate and the soil formation rate (SoF) as follows:

$$NSLow_{year} = (WSi_{year} * f) - (SoF * nyears) \qquad \text{(Eq 4-16)}$$

where f is the conversion factor from $mole.m^{-2}$ to m deep and nyears is the time span considered.

The driving variable of the developed model is acid load (HA, HB, HC) which depends on the SO_2 and CO_2 atmospheric concentrations for each scenario considered.

Based on the acid load entering the soil compartment three different periods of time can be distinguished (see section 2.):

- a period of 330 years, from 1970 to 2300 (estimated exhaustion of fossil fuels) during which the soils are receiving an increasing acid load.

- a short period of time (a few months for SO_2 and some 100 years for CO_2) for the recovery of the background concentration of such gases. The soil compartment receives a decreasing acid load.

- finally, a time span of some 58.000 years up to next Ice Age, where the acid load entering the soil is constant and corresponds to the acidity originated from natural sources.

The model computations are performed separately for each of the above mentioned periods of time.

Increasing acid load: 1970-2300

The annual acid load (moles. m^{-2}. $year^{-1}$) for each scenario is calculated according to Eq 4-17 as follows:

$$HA,B,C_{year} = a*10^3*SO_4^{2-}A,B,C_{year} + 2*10^3*H_2CO_3(aq)_{year} \qquad \text{(Eq 4-17)}$$

where a= 1.33 in soils supporting deciduous stands and a= 2.13 (1.33*1.6) in soils supporting coniferous stands (see Eq 4-4 and section 4.2.2).

The evolution of the annual acid load in forested podzols along this time-span for the three scenarios studied is depicted in Figures 4-3 and 4-4.

The total acid load received by the soil during the period 1970-2300 depending on the scenario studied and the type of afforestation is shown below in Table 4-1.

	Total Acid Load (moles.m^{-2})		
	scenario **A**	scenario **B**	scenario **C**
Deciduous stands	72.0	137.8	403.8
Coniferous stands	109.0	214.2	639.8

Table 4-1. Total acid load received by podzols in Southern Sweden depending on the scenario studied and the type of afforestation during the period 1970-2300.

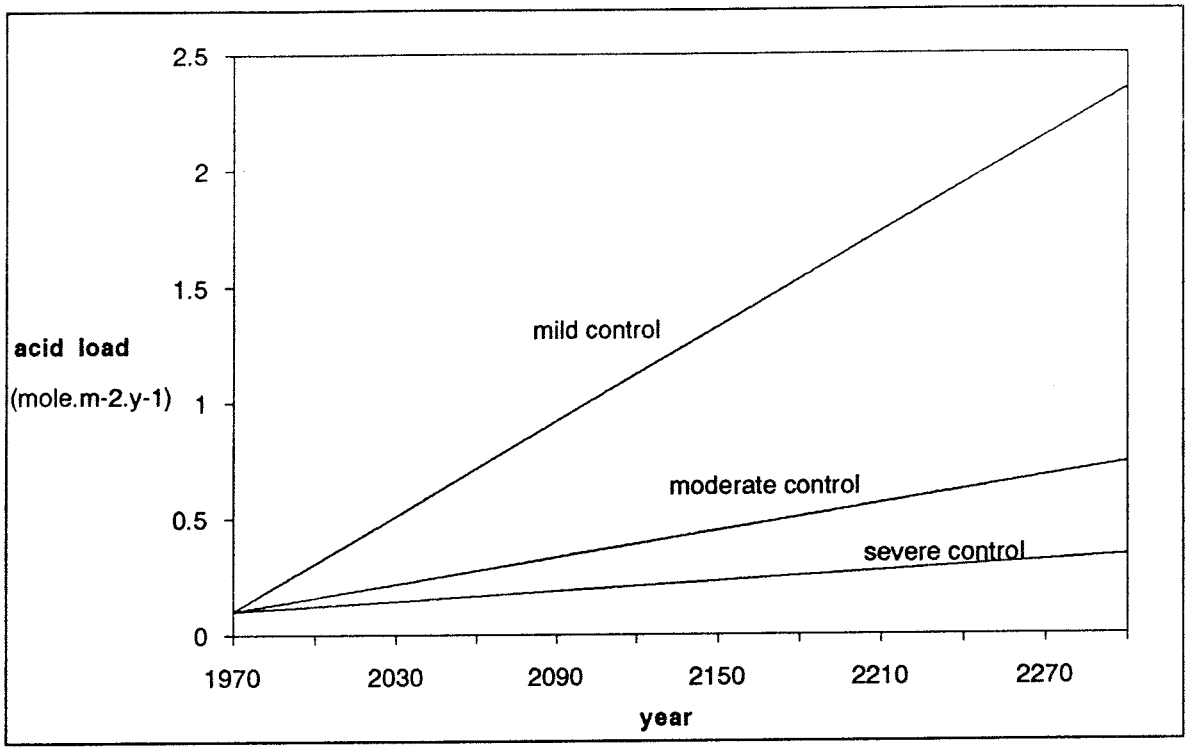

Figure 4-3. Acid load entering soils supporting deciduous forests from 1970 to depletion of fossil fuels (2300) for the three studied scenarios.

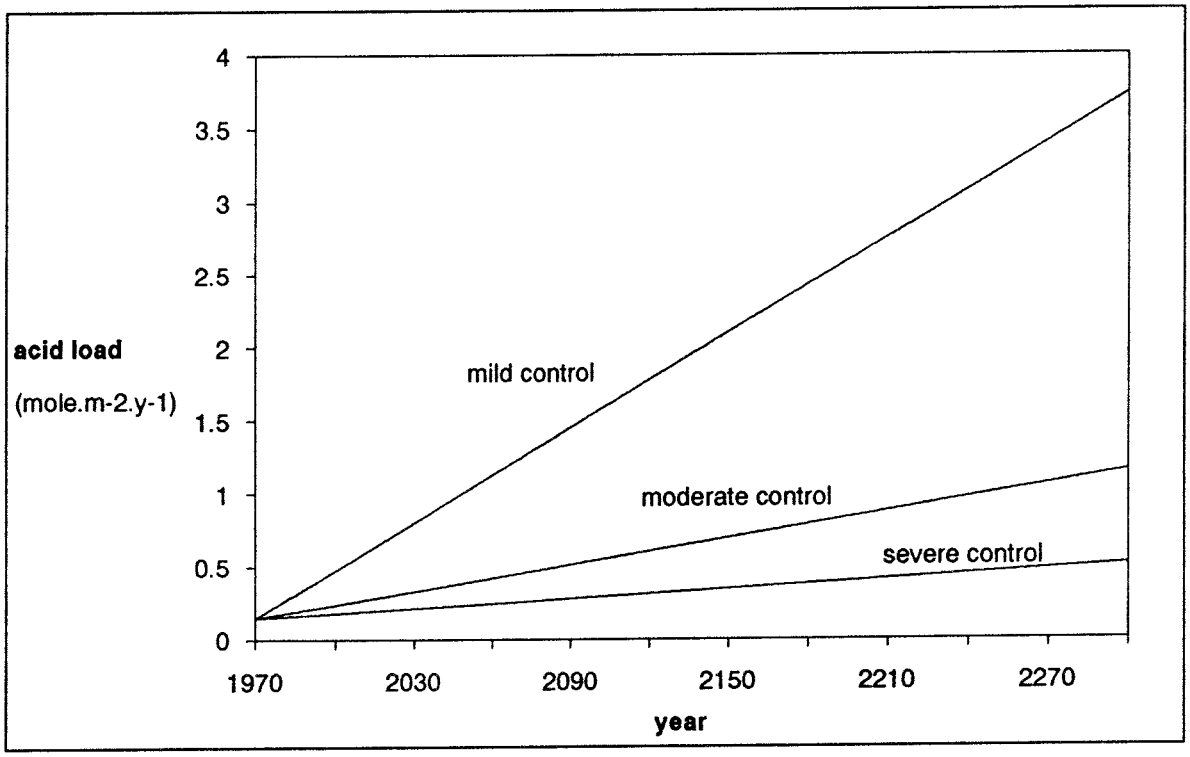

Figure 4-4. Acid load entering soils supporting coniferous forests from 1970 to depletion fossil fuels (2300) for the three studied scenarios.

The variation of the cation exchange buffer capacity with time is calculated according to Eq 4-18.

$$ßCEA,B,C_{year} = ßCE0A,B,C_{year} - (HA,B,C_{year} - brSi) \quad \text{(Eq 4-18)}$$

The evolution of cation exchange buffer capacity and base saturation of the soil during this period of time depending on the afforestation is shown in Figures 4-5, 4-6, 4-7 and 4-8.

The predicted soil pH values under different conditions of afforestation during the period 1970-2300 are shown in Figures 4-9 and 4-10.

As mentioned above, the silicate weathering rate was kept constant through the computations. Once the pH of the soil was calculated, a check of the reliability of this assumption was made.

The silicate weathering rate constant (k_{Si}) was calculated by assuming that the initial weathering rate (0.05 mole.m^{-2}.y^{-1}) was measured at pH= 4.33. By taking into account a 0.5 order kinetics of the silicate weathering rate (Stumm and Wollast, 1990 and references therein), k_{Si} is calculated as:

$$k_{Si} = brSi * (10^{-4.33})^{-0.5} \quad \text{(Eq 4-19)}$$

Therefore, the dependence of silicate weathering rate upon time (or soil acidity) for each scenario can be written as a rate equation as follows:

$$brSiA,B,C_{year} = k_{Si} * (HA,B,C_{year})^{0.5} \quad \text{(Eq 4-20)}$$

The variation of the silicate weathering rate with time (or soil acidity) is depicted in Figures 4-11 and 4-12.

The total amount of silicate weathered (mole.m^{-2}) can be easily calculated by integrating the weathering rate equation (Eq 4-16) within 1970 and 2300, except for the scenario C. In this worst case scenario, the soil cation exchange buffer capacity is exhausted by 2144 in the case of soils supporting deciduous stands, and by 2078 in soils under coniferous forests. The rate equation developed can only be applied within this buffer range and the amount of weathered silicate is computed by this method up to those limits. During next 50 years (see section 4.2.2.) the weathering rate is assumed to remain constant and finally from 2128 (coniferous stands) and 2194 (deciduous stands) the silicate weathering rate is assumed to be the one which applies for the $Al(OH)_3$ buffer range. Table 4-2 shows the weathered silicate during this time span depending on afforestation and scenario.

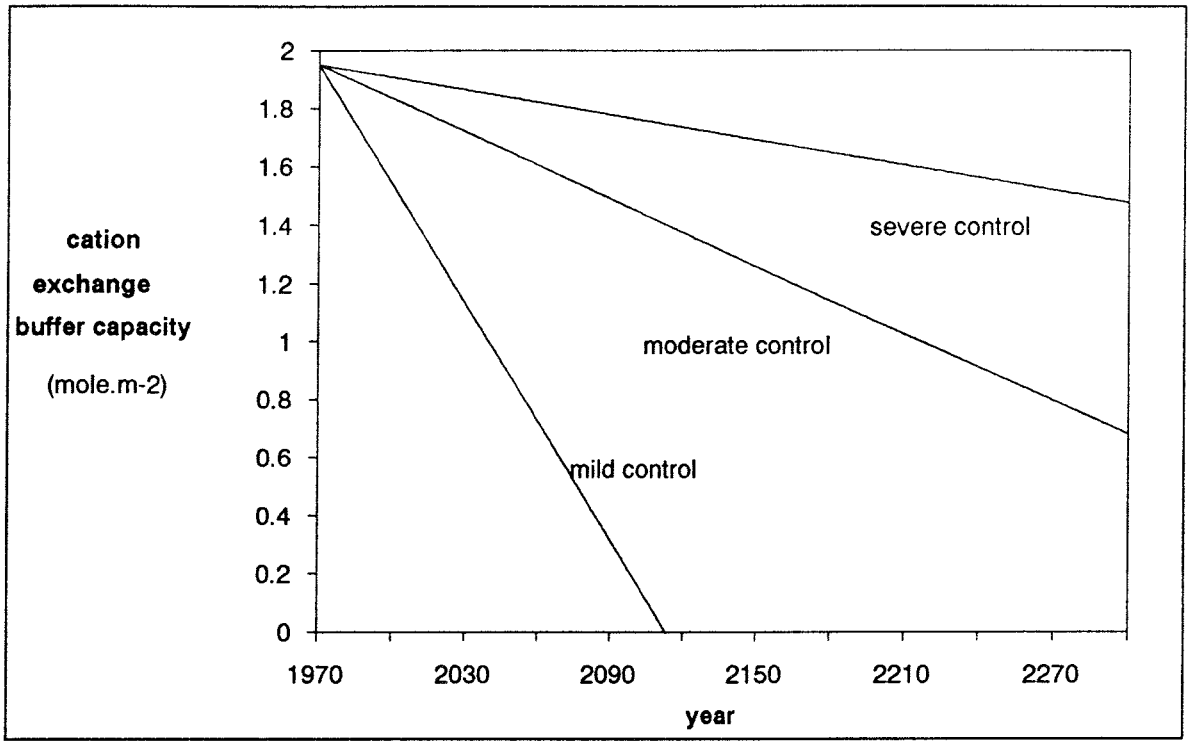

Figure 4-5. Evolution of soil cation exchange buffer capacity in deciduous forests from 1970 to depletion of fossil fuels (2300) for the three studied scenarios.

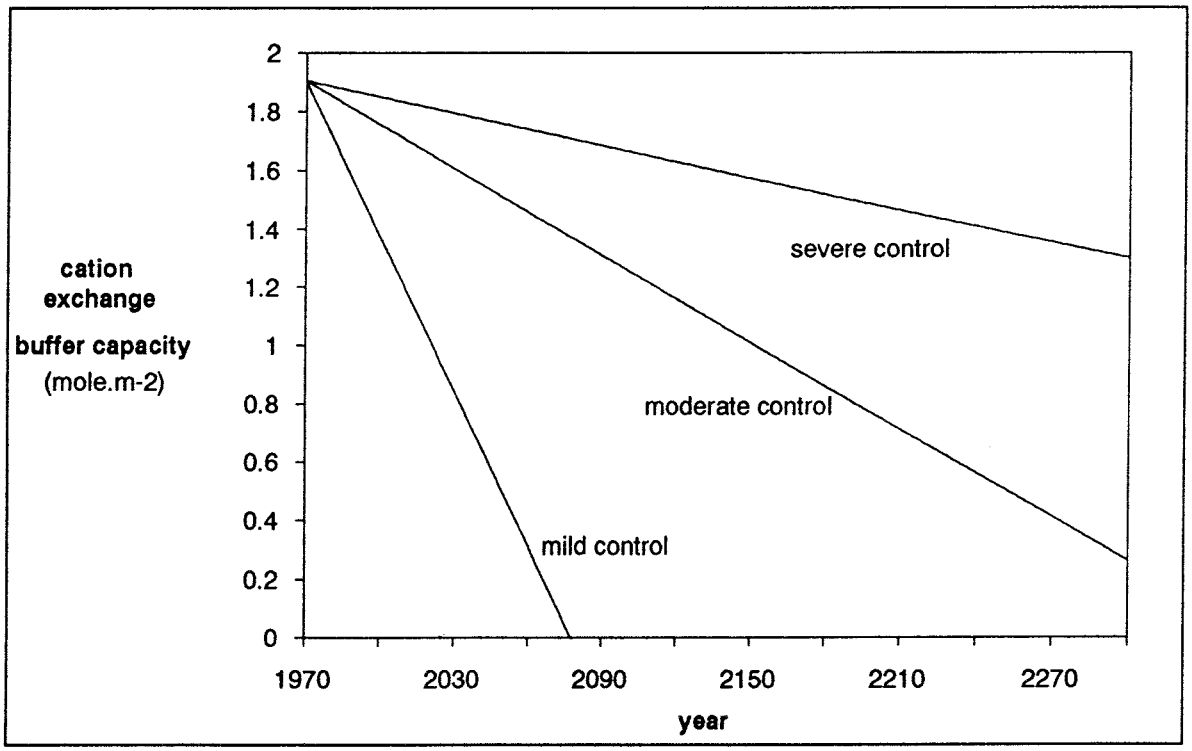

Figure 4-6. Evolution of soil cation exchange buffer capacity in coniferous forests from 1970 to depletion of fossil fuels (2300) for the three studied scenarios.

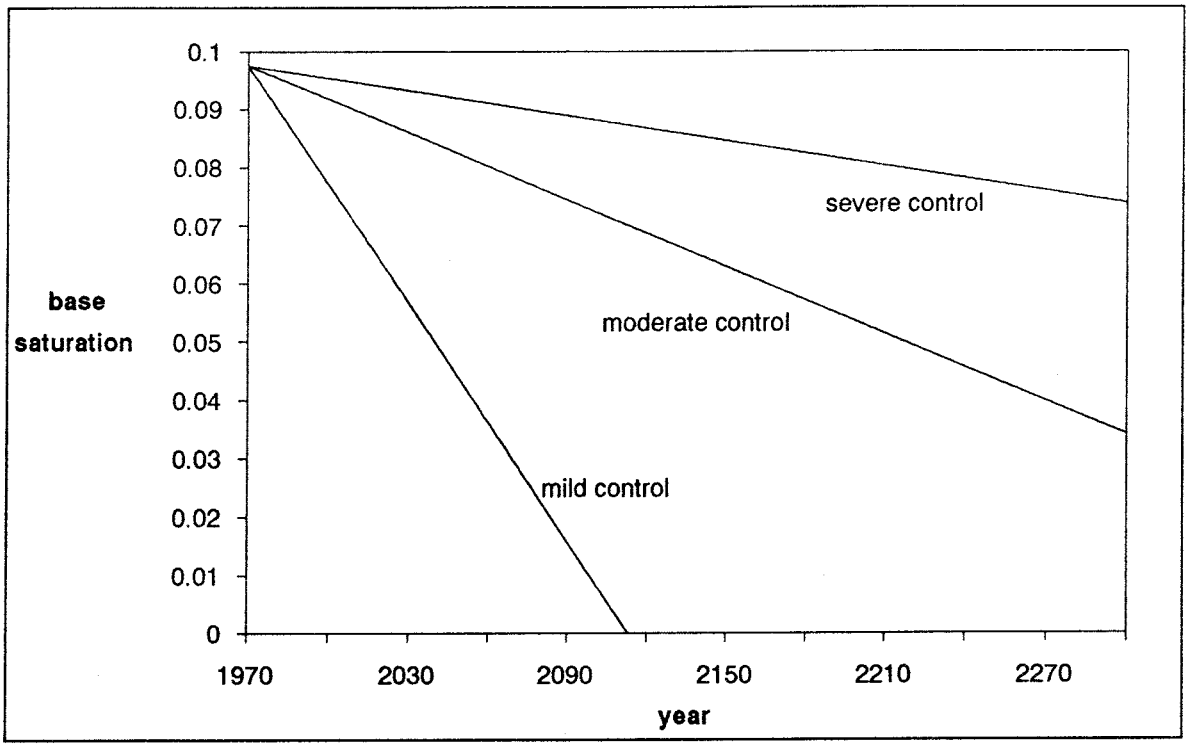

Figure 4-7. Evolution of the base saturation of soils supporting deciduous stands from 1970 to depletion of fossil fuels (2300) for the three studied scenarios.

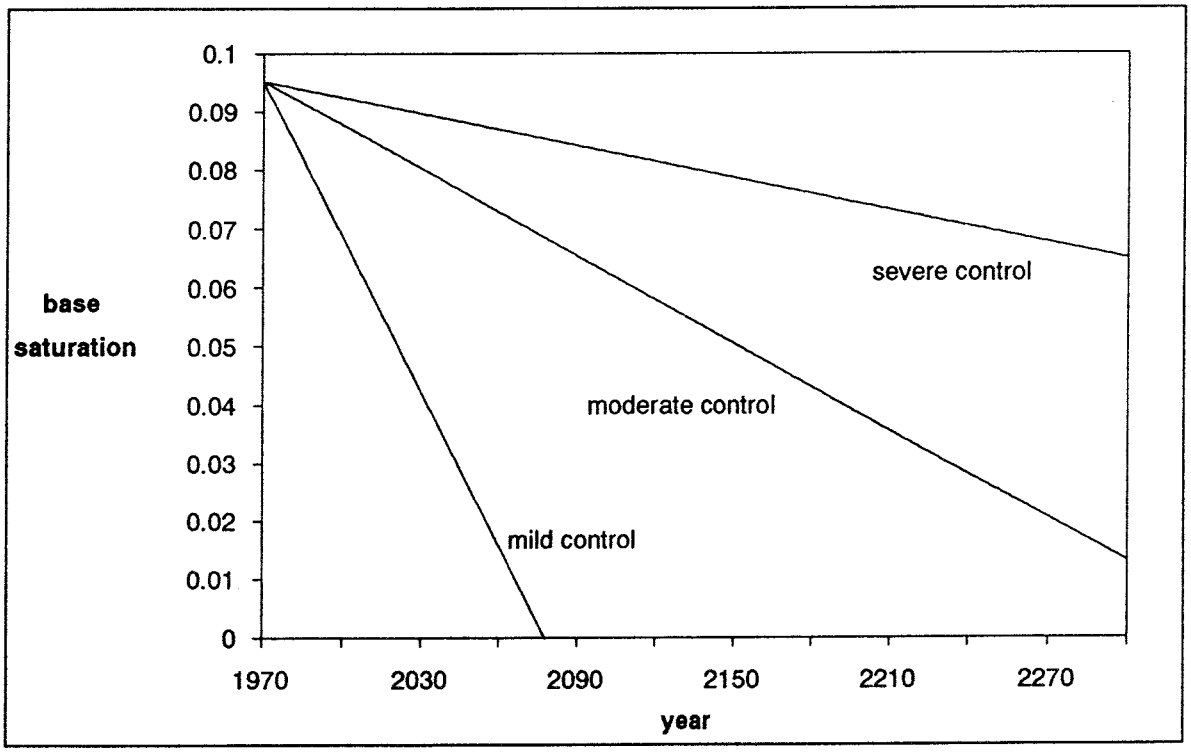

Figure 4-8. Evolution of the base saturation of soils supporting coniferous stands from 1970 to depletion of fossil fuels (2300) for the three studied scenarios.

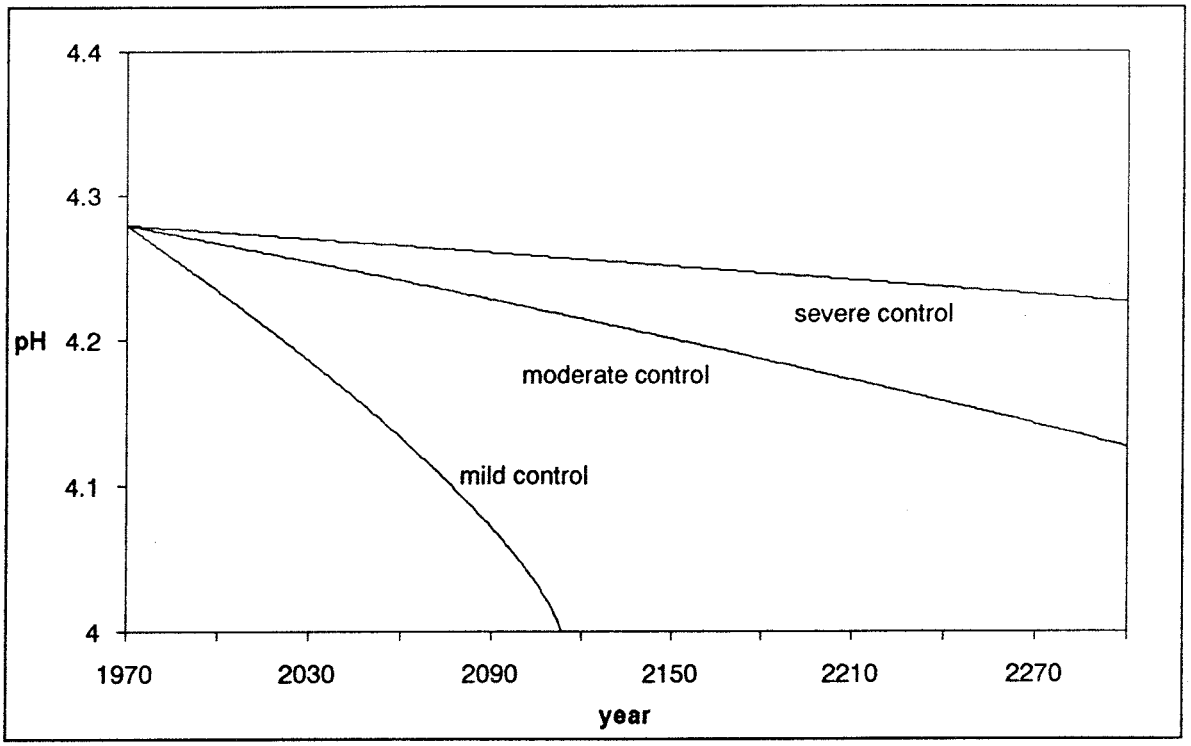

Figure 4-9. Evolution of the pH of soils supporting deciduous forests from 1970 to depletion of fossil fuels (2300) for the three studied scenarios.

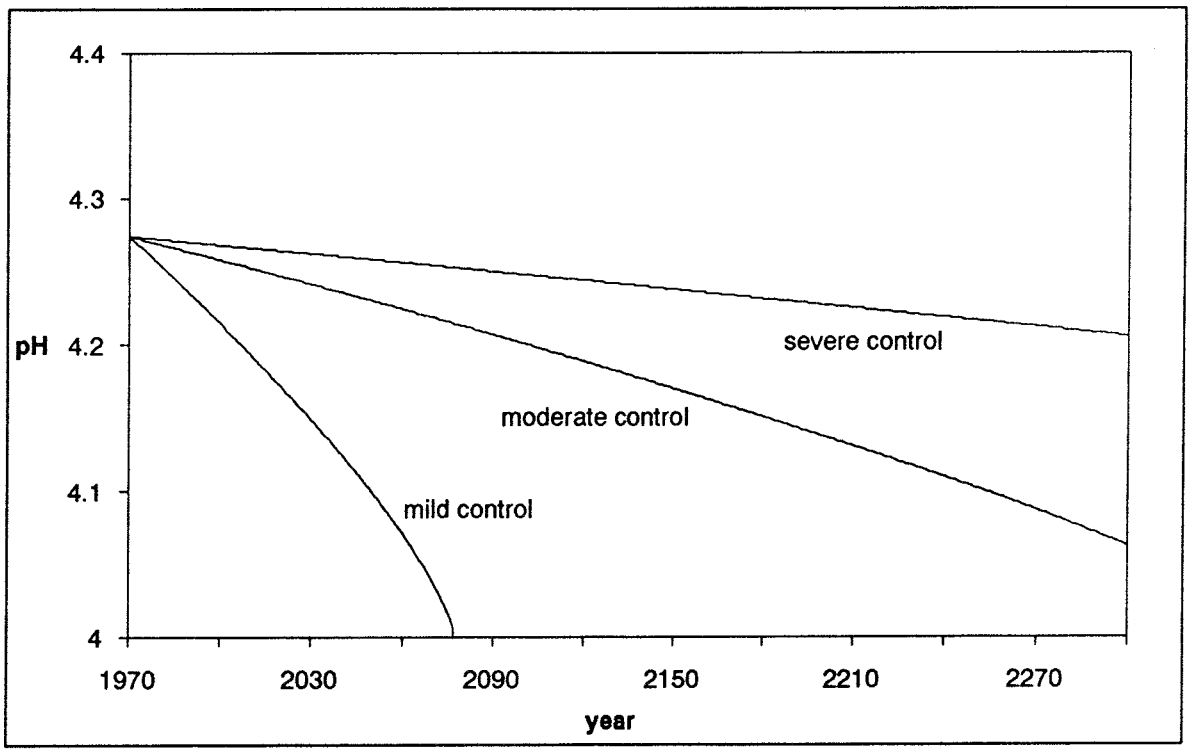

Figure 4-10. Evolution of the pH of soils supporting coniferous forests from 1970 to depletion of fossil fuels (2300) for the three studied scenarios.

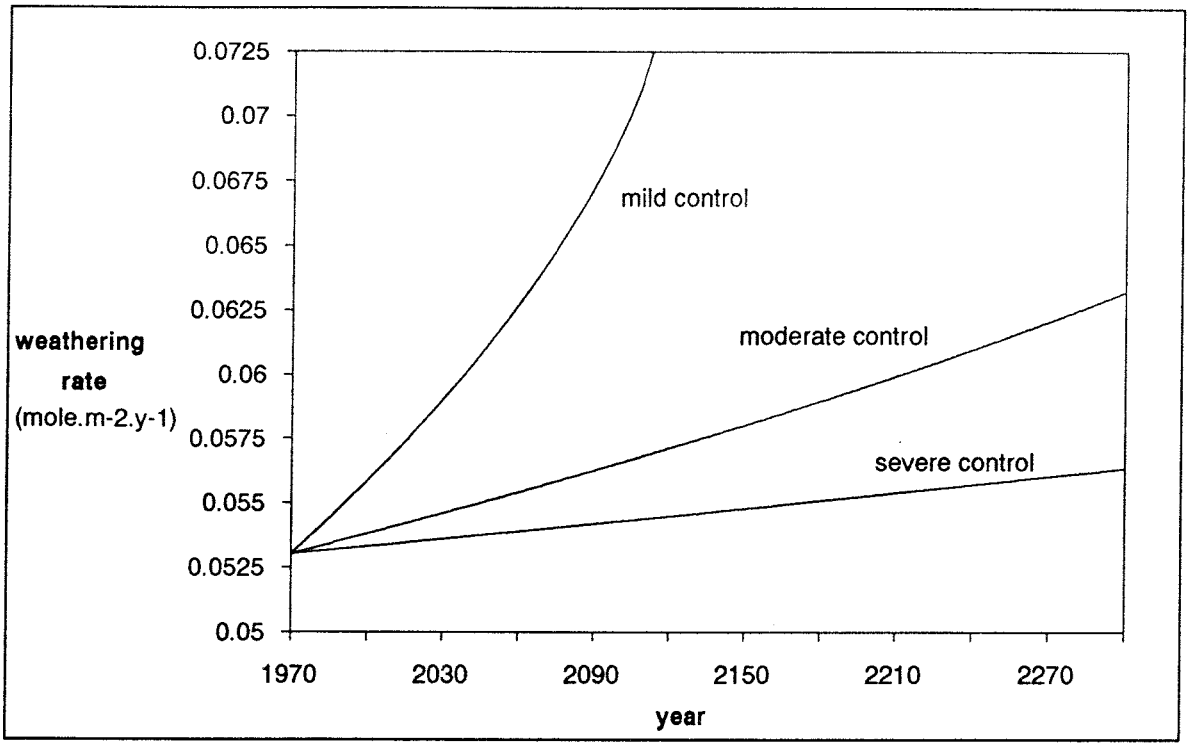

Figure 4-11. Variation of the weathering rate with time (or soil acidity) from 1970 to depletion of fossil fuels (2300) on soils supporting deciduous forests depending on the studied scenario.

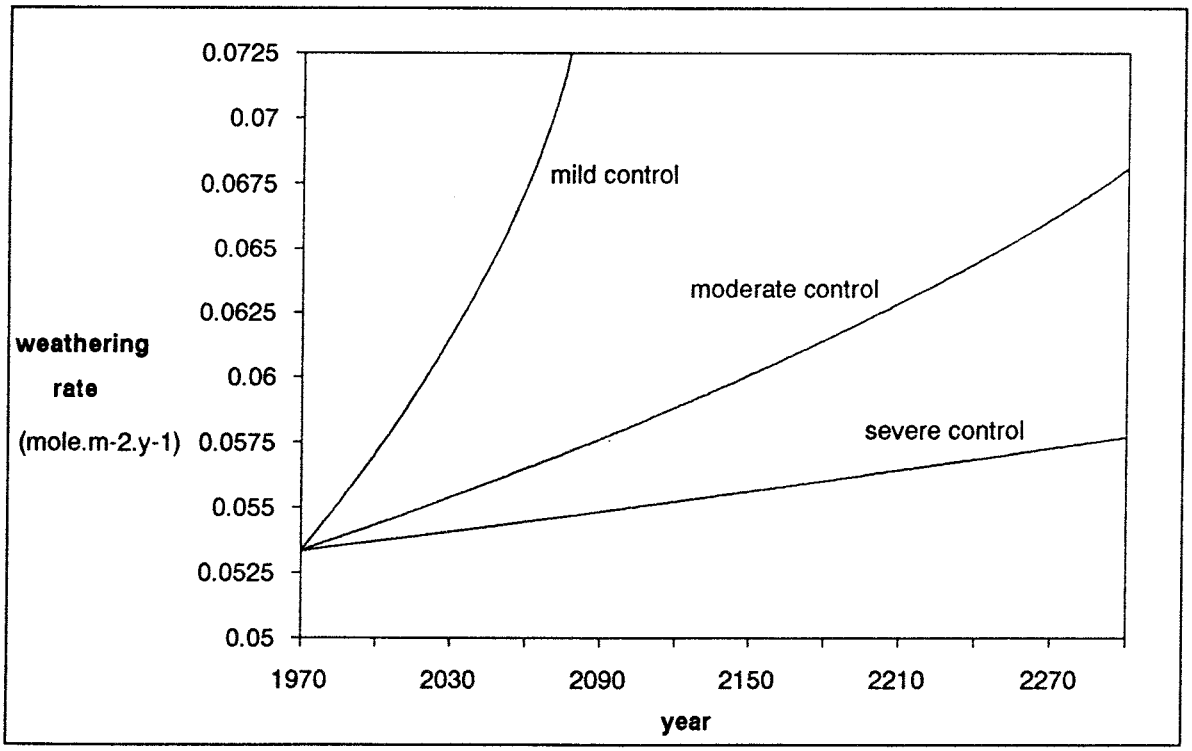

Figure 4-12. Variation of the weathering rate with time (or soil acidity) from 1970 to depletion of fossil fuels (2300) on soils supporting coniferous forests depending on the studied scenario.

	Weathered Silicate (mole.m^{-2})		
	scenario **A**	scenario **B**	scenario **C**
Constant weathering rate: coniferous and deciduous stands	16.5	16.5	16.5
Weathering rate dependent on the pH: deciduous stands	18.0	19.0	227.1 (8.7+3.5+214.9)
Weathering rate dependent on the pH: coniferous stands	18.4	19.9	281.0 (5.6+3.6+271.8)

Table 4-2. Total amount of silicate weathered (in mole.m^{-2}) in forested soils during the period 1970-2300 considering a constant weathering rate (0.05 mole.m^{-2}.y^{-1}) and a weathering rate dependent on the soil pH. In the case of the scenario C, the three terms correspond respectively to the silicate weathered during the period of dominance of the cation exchange buffer range, to the intermediate period during which deforestation proceeds and to the time span where $Al(OH)_3$ dissolution is the dominant buffer reaction.

The net surface lowering is calculated for the scenarios A and B as shown in Eq 4-21.

$$NSLowA,B_{1970\text{-}2300} = (f * WSiA,B_{1970\text{-}2300}) - (SoF * (2300-1970)) \qquad \text{(Eq 4-21)}$$

where f= 1.5*10^{-3}, being the conversion coefficient from silicate weathering rate (mole.m^{-2}.y^{-1}) to surface lowering rate (m.y^{-1}) (see sections 4.2.2 and 4.2.3).

The net surface lowering exploring the scenario C is computed according to Eq 4-22 in three steps depending on the weathering rate.

$$NSLowC_{1970\text{-}2300} = NSLowC_{1970\text{-}year} + (50*brSi_{year}) + ((2300\text{-}50\text{-}year)*brSi_{Al}) \qquad \text{(Eq 4-22)}$$

where year = 2144 in deciduous stands and year = 2078 in coniferous stands.

The calculated net surface lowering by 2300 in Swedish podzols depending on the type of afforestation is shown in Table 4-3.

	Net Surface Lowering (m)		
	scenario A	scenario B	scenario C
Deciduous stands	0.024 (0.022)	0.026 (0.022)	0.34
Coniferous stands	0.024 (0.022)	0.027 (0.022)	0.42

Table 4-3. Expected net surface lowering by 2300 for the studied scenarios depending on the forest stand assuming a weathering rate dependent on soil pH. Figures in brackets denotes the expected surface lowering assuming a constant weathering rate.

Decreasing acid load: 2300-2406

After exhaustion of fossil fuels SO_2 atmospheric concentration returns very rapidly to the pre-industrial background level (1-2 months) (see section 4.1). In the developed model it is considered that SO_2, as sulphate, accounts during this period for a constant acid load into the soil corresponding to the background sulfur cycling.

Eq 2-6 and 4-5 describing the decay of atmospheric CO_2 from 2300 on and the solubility of CO_2 in rainwater are used to calculate the annual concentration of dissolved CO_2 ($H_2CO_3(aq)$) according to Eq 4-23.

$$H_2CO_3(aq)_{year} = H_2CO_3(aq)_{2300} * e^{-0.007*(year-2300)} \qquad \text{(Eq 4-23)}$$

Hence, the acid load received by the soil can be calculated as indicated by Eq 4-24.

$$H_{year} = a*10^3*SO_4^{2-}{}_{backg} + 2*10^3*H_2CO_3(aq)_{year} \qquad \text{(Eq 4-24)}$$

where a = 1.33 in deforested soils (scenario C) or soils supporting deciduous stands and a = 2.13 in soils supporting coniferous stands.

The evolution of the annual acid load entering the soil during this time span is shown in Figure 4-13.

The soil cation exchange buffer capacity in the scenarios A and B is computed as in the previous period, by using the Eq 4-25.

$$\text{ßCEA,B}_{year} = \text{ßCEA,B}_{year-1} - (\text{HA,B}_{year}\text{-brSi}) \qquad \text{(Eq 4-25)}$$

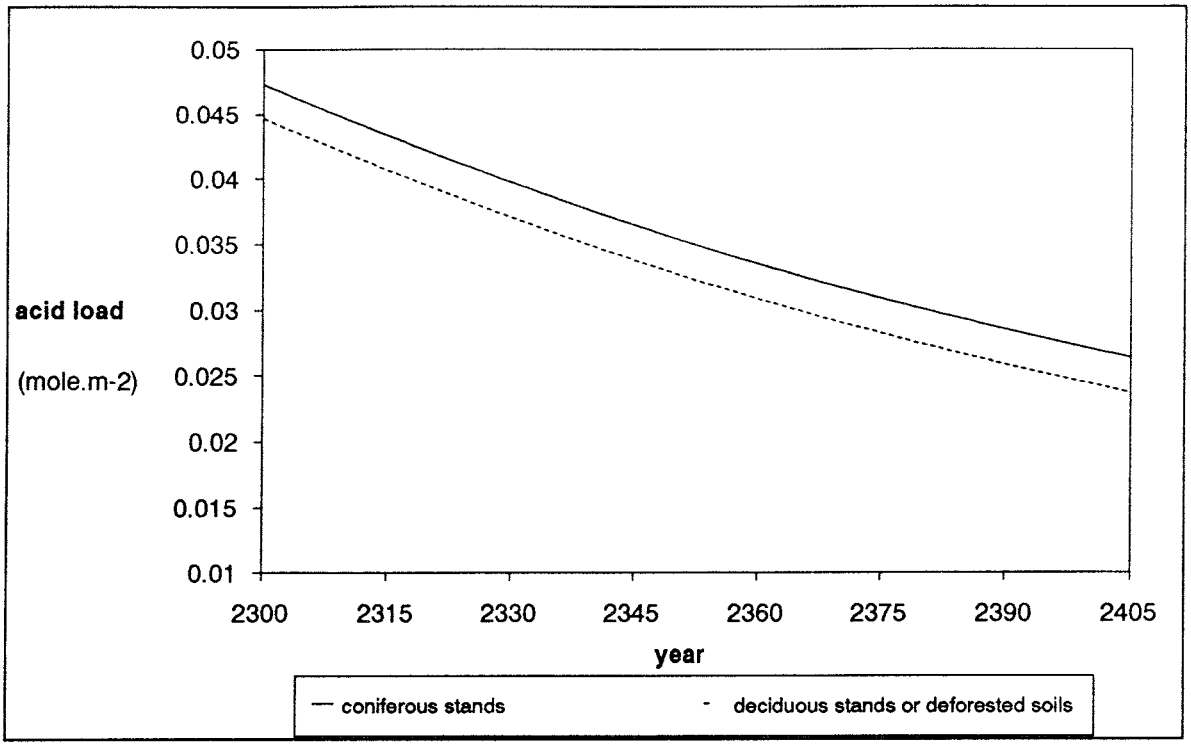

Figure 4-13. Evolution of the acid load entering the soil in the scenarios A and B depending on the type of afforestation during the period of decay of CO_2 atmospheric concentration (2300-2406).

The variation of the soil cation exchange buffer capacity and base saturation with time within the scenarios A and B is depicted in figures 4-14 and 4-15.

The pH of the soil for the scenarios A and B is again calculated from the above mentioned Reuss' non-linear relationship (Eq 4-15). The evolution of the soil pH for the scenarios A and B during this period is depicted in figure 4-16.

Since it has been previously shown that for the scenarios A and B, only a slight increase on the silicate weathering rate can be expected as a consequence of the increased activity of hydrogen ions in the soil solution, the total amount of silicate weathered during the decay period is calculated assuming the weathering rate to be constant (brSi).

In the worst case scenario (C), the amount of weathered silicate is computed by using the weathering rate corresponding to the aluminum buffer range ($brSi_{Al}$).

The net surface lowering corresponding to this period is calculated for the scenarios A and B as was from 1970 to 2300. For the scenario C, it is computed according to Eq 4-26, assuming no formation of soil subsequent to weathering of silicate minerals (see section 4.2.2).

$$NSLowC_{2300\text{-}2406} = f * WSiC_{2300\text{-}2406} \qquad \text{(Eq 4-26)}$$

The total amount of silicate weathered and the corresponding net surface lowering from 2300 to 2406 for the three explored scenarios is shown in Table 4-4.

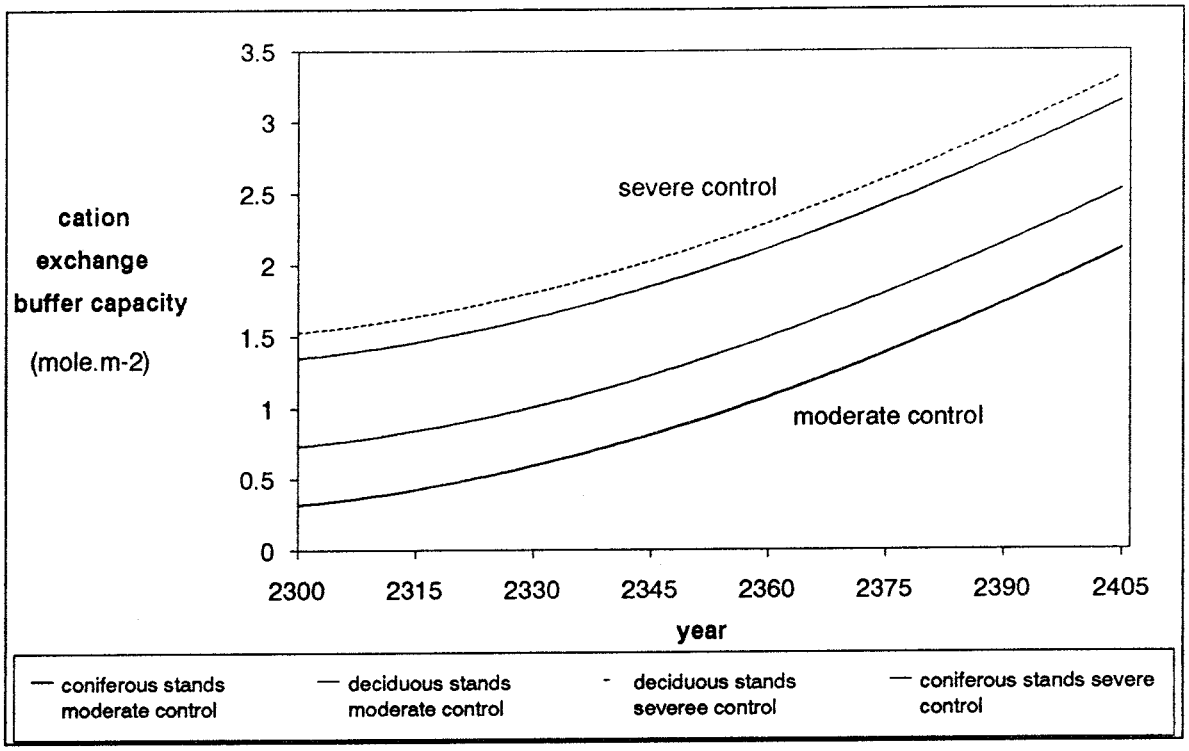

Figure 4-14. Evolution of the soil cation exchange buffer capacity in the scenarios A and B depending on the type of afforestation during the period of decay of CO_2 atmospheric concentration (2300-2406).

	scenarios A,B	scenario C
Acid Load (mole.m^{-2})	3.0	3.0
Weathered Silicate (mole.m^{-2})	5.3	167.5
Net Surface Lowering (m)	0.007	0.4

Table 4-4. Acid load, amount of weathered silicate and net surface lowering from exhaustion of fossil fuels to the recovery of CO_2 background concentration for the three studied scenarios.

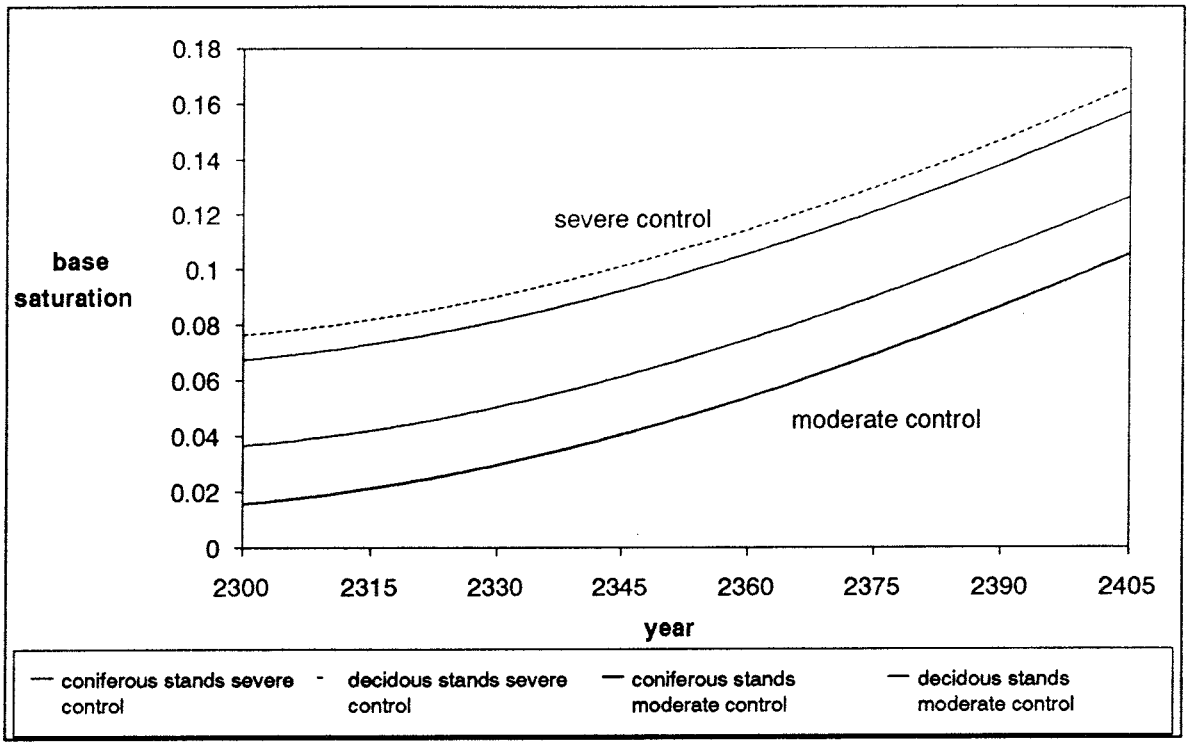

Figure 4-15. Evolution of soil base saturation in the scenarios A and B depending on the type of afforestation during the period of decay of CO_2 atmospheric concentration (2300-2406).

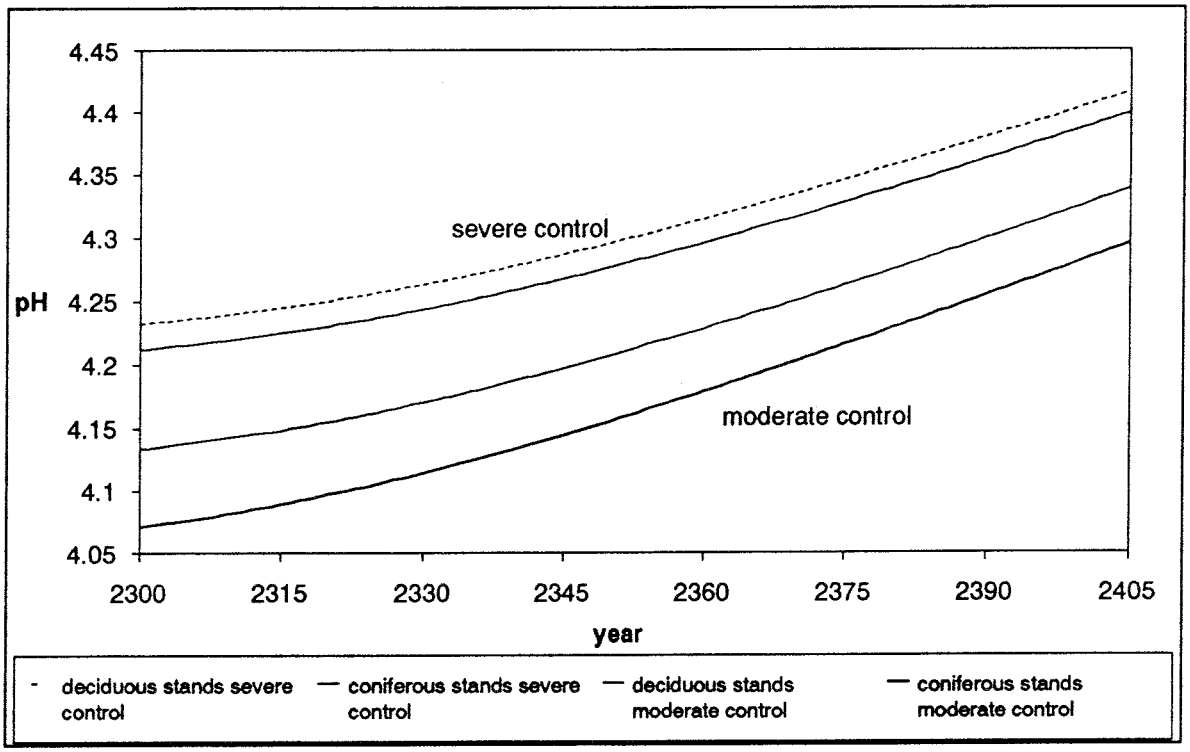

Figure 4-16. Evolution of the soil pH in the scenarios A and B depending on the type of afforestation during the period of decay of CO_2 atmospheric concentration (2300-2406).

Constant acid load from natural sources: 2406-60.000 (Next Ice Age)

The acid input to the soil-bedrock system during this time-span is assumed to be constant and in our model corresponds to 1860 atmospheric concentrations of SO_2 and CO_2. The annual acid load is computed according to Eq 4-27 giving a result of 0.024 mole.m^{-2}.y^{-1}.

$$H_{year} = 1.33*10^3*SO_4^{2-}{}_{backg} + 2*10^3*H_2CO_3(aq)_{backg} \qquad \text{(Eq 4-27)}$$

The annual cation exchange buffer capacity is computed for the scenarios A and B as in the preceding periods according to Eq 4-9. The evolution of the soil cation exchange buffer capacity and soil base saturation in the most favorable scenarios (A and B) are shown in Figures 4-17 and 4-18.

In these favorable scenarios, the soil pH is calculated as in previous periods (Eq 4-15) and its evolution with time is depicted in Figure 4-19.

Table 4-5 below shows the amount of weathered silicate and the net surface lowering from recovery of background concentrations up to next Ice Age depending on the scenario considered.

The global results of acid load, weathered silicate and net surface lowering (1970 to next Ice Age) of the developed model for each of the studied scenarios are shown in Table 4-6.

	scenarios **A,B**	scenario **C**
Acid Load (mole.m^{-2})	$1.38*10^3$	$1.38*10^3$
Weathered Silicate (mole.m^{-2})	$2.88*10^3$	$9.1*10^4$
Net Surface Lowering (m)	3.8	136.5

Table 4-5. Acid load received by Swedish podzols from 2406 up to next Ice Age. Amount of weathered silicate and corresponding expected surface lowering depending on the scenario explored.

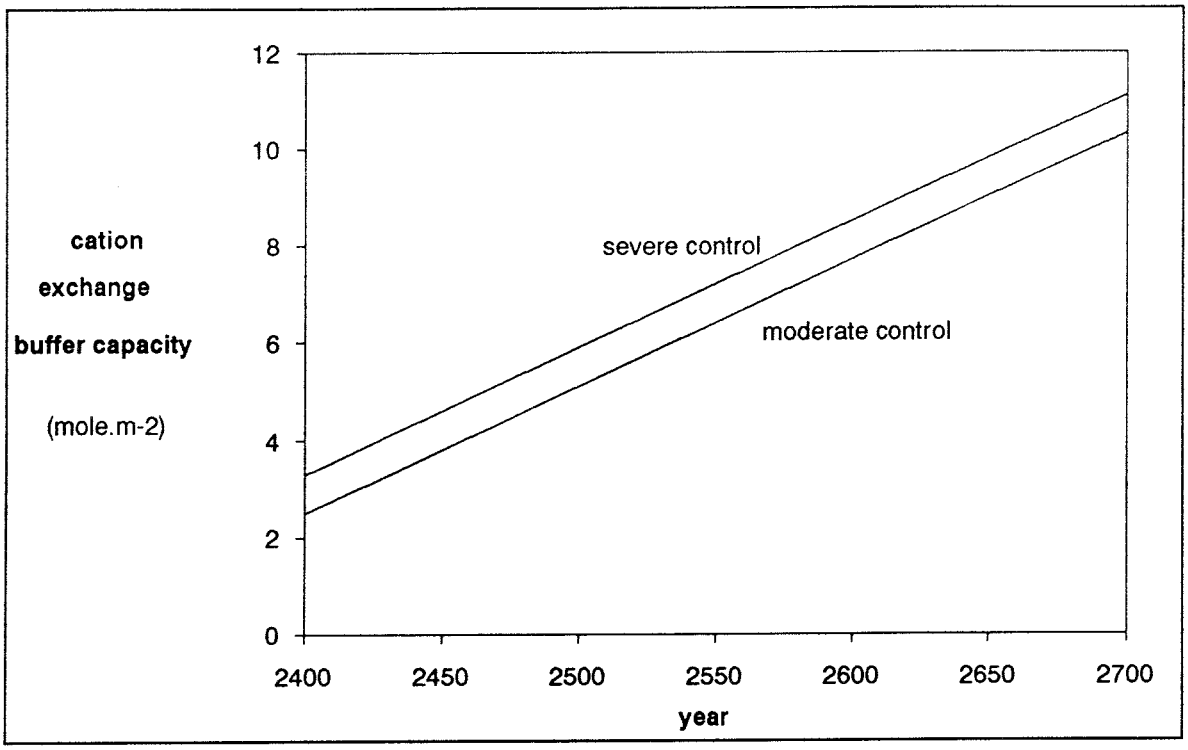

Figure 4-17. Evolution of soil cation exchange buffer capacity from the recovery of background atmospheric concentrations of CO_2 on for the scenarios A and B.

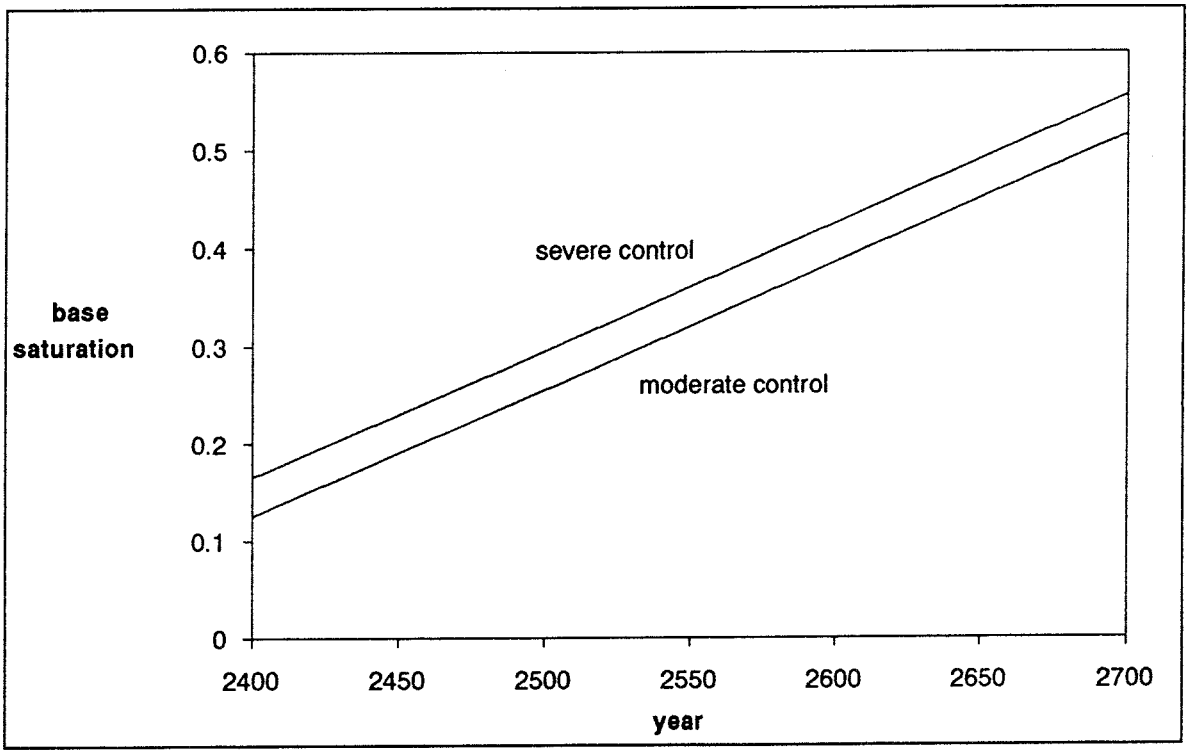

Figure 4-18. Evolution of the base saturation of the soil from the recovery of background atmospheric concentrations of CO_2 on for the scenarios A and B.

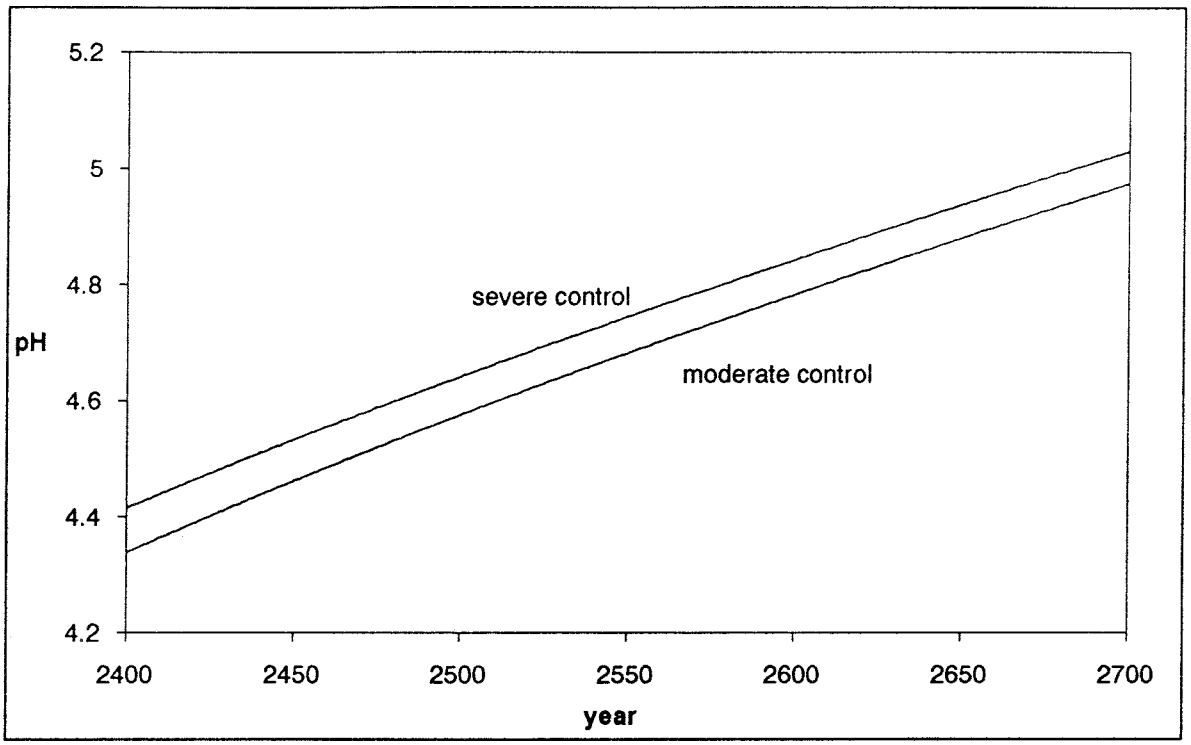

Figure 4-19. Evolution of the pH of the soil from the recovery of background atmospheric concentrations of CO_2 on for the scenarios A and B.

	scenario **A**	scenario **B**	scenario **C**
Total Acid Load (mole.m^{-2})			
deciduous forests	$1.46*10^3$	$1.52*10^3$	$1.79*10^3$
coniferous forests	$1.49*10^3$	$1.60*10^3$	$2.02*10^3$
Total Weathered Silicate (mole.m^{-2})	$2.9*10^3$	$2.9*10^3$	$9.14*10^4$
Total Net Surface Lowering (m)	3.8	3.8	137.1
Soil buffer range by the recovery natural levels CO_2, SO_2	cation exchange	cation exchange	$Al(OH)_3$

Table 4-6. Total acid load received by forested podzols from 1970 to next Ice Age depending on the explored scenario. Estimated amount of silicate weathered, expected surface lowering and soil dominant buffer reaction after recovery of background concentrations of atmospheric SO_2 and CO_2 .

5. SUMMARY AND CONCLUSIONS

As mentioned above, there are two ways in which environmental acidification could have an impact on the planned HLNW repositories. In this report we have focussed on the effects on the geological stability of the bedrock.

A central scenario related to the combustion of fossil fuels for energy is explored. Sulfur dioxide emissions resulting from the use of these fuels are considered to be responsible for the acidification processes. It is also taken into account the expected global build-up of CO_2 concentration in the atmosphere.

Three different sub-scenarios are studied depending on how stringent SO_2 emission controls might be during next centuries: mild control (scenario A), moderate control (scenario B) or severe control (scenario C). A linear increase of varying slope is thought to be the most realistic approach to model the evolution of the atmospheric SO_2 and CO_2 concentrations.

For the scenarios A and B the depth of weathered bedrock is calculated by using the silicate weathering rate corresponding to the cation exchange buffer range. In the worst case scenario (C), the amount of weathered host rock is computed by using the silicate weathering rate corresponding to the aluminum buffer range.

The main conclusions of the model calculations performed along the previous chapter are:

- Due to the short residence time in the atmosphere of SO_2, the time required to restore atmospheric background concentrations is short. This means that any global reduction on the emissions has an immediate effect on the various reservoirs. The behavior of CO_2 is rather different due to its longer residence time. The appropriate reduction measures would have effect only one century later.

- The average atmospheric concentration for the scenario C is respectively 7 and 2.5 times larger than for scenarios A and B. However, the resulting acid load introduced into the soil up to next Ice Age is only a 20% larger in the worst case scenario (C). This is mainly due to the fact that the anthropogenic perturbation lasts for only 0.5% of the total time covered in these calculations.

- There is a well defined threshold for soil acidification, when the cation exchange capacity is depleted. In our calculations this would only happen in the worst case scenario (C). However, for the average case scenario (the one actually operating in Scandinavia), the degree of acidification has a dependence on the type of afforestation. At the end of the "fossil fuel age" (2300), for deciduous forests the pH of the soil is expected to decrease to regional average values around 4.2. In the case of soils under coniferous stands, the pH is expected to decrease down to 4.05. What is more important, the remaining cation exchange buffer capacity ranges from 5% for deciduous forests to only 1% for the coniferous ones.

These are extremely low values for a buffer capacity to be effective and irreversible damage could be expected even in the average case scenario, particularly for podzolic soils supporting coniferous forests. As a matter of fact, larger sensitivity to acidification has been observed in coniferous forests (Johnson and Siccama, 1983).

- In the scenarios A and B the total weathering is only slightly affected by the differences in soil acidity. Over the acid load threshold value (total exhaustion of the cation exchange buffer capacity), the weathering rates are largely increased and so it is the resulting total weathering (case C). This a consequence of a major disruption in the soil structure and the larger availability of wetted surface.

- The net surface lowering resulting from scenarios A and B is only around 4 meters up to next Ice Age. This amounts only to 1% of the depth of the repository (500 meters).

In the worst case scenario, the computed net surface lowering amounts to some 140 meters (between 25 and 30% of the total repository depth). As we have already discussed, this is the result of a large acidification, extensive deforestation and consequently increased weathering rates. The net result of this scenario would be that the Scandinavian ecosystem would become hardly habitable and the performance of the HLNW repository a lesser problem for the biosphere.

However, the increased weathering results in general in a larger penetration of the acidified surface waters into the undisturbed groundwater system. This could possibly have larger implications in the performance of the HLNW repository. These implications will be discussed in a forthcoming report in this series.

The main consequence of this study is that an expanded usage of fossil fuels without the pertinent emissions control could affect the already stressed Swedish ecosystem. This has to be kept in mind when balancing different energy alternatives and their related cycles.

6. REFERENCES

AHLBOM, K., ÄIKÄS, T., ERIKSSON, L.O. (1990)
SKB/TVO Ice Age Scenario.
SKB Technical report.

ALCAMO, J., SHAW, R., HORDIJK, L. (eds.)(1989)
The rains model of acidification.
Kluwer Academic Publishers, Dordrecht.

BARTH, T. F. W. (1961)
Abundance of the elements, areal averages and geochemical cycles.
Geochim. Cosmochim. Acta **23**, 1-8.

BERDEN, M., INGVAR NILSSON, S., ROSEN, K., TYLER, G. (1987)
Soil Acidification, extent, causes and consequences.
Report 3292, National Swedish Environment Protection Board.

BRICARD, J. (1977)
Aerosol production in the atmosphere. In: J. O'M. Bockris (ed.) Environmental Chemistry. Plenum Press, New York. p. 313-330.

GIBBONS, J.H., BLAIR, P.D., GWIN, H.L.
Strategies for energy use.
Scientific American **261**(3), 86-93.

GRAEDEL, T.E., CRUTZEN, P.J. (1989)
The changing atmosphere.
Scientific American **261**(3), 28-36.

HORDIJK, L., SHAW, R., ALCAMO, J. (1989)
Background to acidification in Europe. In: J. Alcamo, R. Shaw and L. Hordijk (eds.). The Rains model of acidification. Kluwer Academic Publishers, Dordrecht, p. 31-60.

JACKS, G., KNUTSSON, G., MAXE, L., FYLKNER, A. (1984)
Effect of acid rain on soil and groundwater in Sweden.
In: B. Yaron, G. Dagan and J. Goldshmid eds. Pollutants in Porous Media. Springer-Verlag, p. 94-114.

JACOBSON, J.S. (1978)
Experimental studies on the phytotoxicity of acidic precipitation.In: T.C. Hutchinson, M. Havas (eds.). NATO Conference on effects of acid precipitation on vegetation and soils (Toronto, 1978). Plenum Press, p. 151-160.

JOHNSON, A.H., SICCAMA, T.G. (1983)
Acid deposition and forest decline.
Environ. Sci. Technol. **17**(7), 294-305.

JOHNSON, A.H., SIGG, L. (1985)
Acidity of rain and fog: conceptual definitions and practical measurements.
Chimia **39**, 59-61.

JOHNSON, N.M., REYNOLDS, R.C. (1972)
Atmospheric sulfur: its effect on the chemical weathering in New England.
Science **117**, 514-516.

KAUPPI, P., ALCAMO, J. (1989)
Modelling soil acidification in Europe. In: J. Alcamo, R. Shaw and L. Hordijk (eds.) The Rains model of acidification. Kluwer Academic Publishers, Dordrecht, p. 179-221.

KAUPPI, P., ALCAMO, J. (1989)
Linkages in the Rains model. In: J. Alcamo, R. Shaw and L. Hordijk (eds.) The Rains model of acidification. Kluwer Academic Publishers, Dordrecht, p. 297-317.

LERMAN, A. (1988)
Weathering rates and major transport processes. An introduction. In: A. Lerman and M. Meybeck (eds.) Physical and chemical weathering in geochemical cycles. NATO ASI Series. Kluwer Academic Publishers, Dordrecht, p. 1-10.

LIKENS, G.E., WRIGHT, R.F., GALLOWAY, J.N., BUTLER, T.J. (1979)
Acid rain.
Scientific American **241**(4), 39-47.

MÄKELÄ, A., SCHOPP, W. (1989)
Regional-scale SO_2 forest impact calculations. In: J. Alcamo, R. Shaw and L. Hordijk (eds.) The Rains model of acidification. Kluwer Academic Publishers, Dordrecht, p.263- 296.

MAYER, R., ULRICH, B. (1978)
Input to soil, especially the influence of vegetation in intercepting and modifying inputs - A review. In: T.C. Hutchinson, M. Havas (eds.). NATO Conference on effects of acid precipitation on vegetation and soils (Toronto, 1978). Plenum Press, p. 173-182.

McLEOD, A.R., HOLLAND, M.R., SHAW, P.J.A., SUTHERLAND, P.M., DARRALL, M.N., SKEFFINGTON, R.A.
Enhancement of nitrogen deposition to forest trees exposed to SO_2.
Nature **347**, 277-279.

PACES, T. (1986)
Weathering rates of gneiss and depletion of exchangeable cations in soil under environmental acidification.
J Geol Soc London **143**, 673-677.

OWENS, L.B., WATSON, J.P. (1979a)
Rates of weathering and soil formation on granite in Rhodesia.
Soil Sci. Soc. Am. J. **43**, 160-166.

OWENS, L.B., WATSON, J.P. (1979b)
Landscape reduction by weathering in small Rhodesian watersheds.
Geology **7**, 281-284.

RAISWELL, R.W., BRIMBLECOMBE P., DENT, D.L., LISS, P.S. (1983)
Química Ambiental. Ediciones Omega S.A., Barcelona.

REUSS, J.O. (1983)
Implications of the calcium-aluminum exchange system for the effect of acid precipitation on soils.
J. Environ. Qual. **12**(4), 591-595.

RODHE, H., GRANAT, L., SÖDERLUND, R. (1984a)
Sulphate in precipitation. A presentation of data from the European Air Chemistry Network. Report CM-64, Dept. of Meteorology of University of Stockholm and International Meteorological Institute of Stockholm.

RODHE, H., GRANAT, L. (1984b)
An evaluation of sulphate in european precipitation 1955-1982.
Atmospheric Environment **18**(12), p. 2627-2639.

RODHE, H., ROOD, M.J. (1986)
Temporal evolution of nitrogen compounds in Swedish precipitation since 1955.
Nature **321**, 762-764.

SCHNEIDER, S.H. (1989)
The changing climate.
Scientific American **261**(3), 38-47.

SCHNOOR, J.L. (1990)
Kinetics of chemical weathering: a comparison of laboratory and field weathering rates. In: W. Stumm (ed.) Aquatic chemical kinetics. Wiley & sons Inc.

SEKIHARA, K. (1977)
Possible climatic changes from carbon dioxide increase in the atmosphere. In: J. O'M. Bockris (ed.) Environmental Chemistry. Plenum Press, New York. p. 285-311.

SEMB, A.(1978)
Sulfur emissions in Europe.
Atmos. Environ. **12**, 455-460.

SLAYMAKER, O. (1988)
Slope erosion and mass movement in to weathering in geochemical cycles. In: A. Lerman and M. Meybeck (eds.) Physical and chemical weathering in geochemical cycles. NATO ASI Series.

SÖDERLUND, R., GRANAT, L. (1981)
Sodium in precipitation. A presentation of data from the European Air Chemistry Network. Report CM-54, Dept. of Meteorology of Univ. of Stockholm and Intl. Meteorological Institute of Stockholm.

STUMM, W., WOLLAST, R. (1990)
Coordination chemistry of the weathering.
Reviews of Geophysics, 1990.

TANKE, M., GULIK, J. v. (1989)
The global climate. Mirage Publishing, Amsterdam.

TOMLISON II, G.H. (1983)
Air pollutants and forest decline.
Environ. Sci. Technol. **17**(6), 246-256.

WAYNE, R.P. (1985)
Chemistry of Atmospheres. Oxford University Press, New York.

WHITE, G.N., FELDMAN, S.B., ZELAZNY, L.W. (1990)
Nutrient release by mineral weathering. In: A. Lucier and S. Haynes (eds.) Mechanisms of forest response to acidic deposition. Springer-Verlag, New York.

WOLT, J.D. (1990)
Effects of acidic deposition on the chemical form and bioavailability of soil aluminum and manganese. In: A. Lucier and S. Haynes (eds.) Mechanisms of forest response to acidic deposition. Springer-Verlag, New York.

WRIGHT, R.F. (1988)
Influence of acid rain on weathering rates. In: A. Lerman and M. Meybeck (eds.) Physical and chemical weathering in geochemical cycles. NATO ASI Series. Kluwer Academic Publishers, Dordrecht, p. 181-196.

7. ACKNOWLEDGEMENTS

This work has been financed by SKB (Swedish Nuclear Fuel and Waste Management). We are very indebted to Dr. Peter Wikberg for his encouragement and support.

APPENDIX A. Selected stations to calculate the average total sulphate content in precipitation in Central and Southern Sweden. Median excess sulphate and sodium concentrations ($\mu mole.dm^{-3}$) (Rodhe et al., 1984a and Söderlund et al, 1981).

STATION NUMBER	STATION NAME	SO42- median value	Na+ median value
16	KVARNTOR	98.1	20.6
21	FLAHULT	65.7	23.5
23	PLÖNNING	109.0	79.6
32	SKURUP	120.0	55.1
38	GÖTEBORG	160.0	131.0
39	STOCKHOLM	176.0	33.4
40	BOHUSMAL	97.2	336.0
42	RYDAKUNG	76.6	12.4
43	UPPSALAN	96.8	19.3
44	KLUNKHYT	92.1	17.4
46	FÄRNABRU	91.7	12.9
47	BJÖRSUND	83.4	14.1
48	TÄRNA	90.0	14.5
51	AS	76.6	24.6
80	SJÖÄNGEN	73.0	17.0
124	ARUP	98.1	23.5
126	GRANAN	81.6	28.0
128	KOMOSSE	72.8	42.7
131	SODERARM	116.0	125.0
133	GRIMSÖ	77.4	11.1
134	KALLANDS	69.5	15.0
135	AKERSHUS	84.7	23.3
136	TORSÖ	66.2	10.1
137	VÄSE	83.0	18.9

APPENDIX B. List of symbols used and correspondence with the symbolism used in the RAINS model.

PARAMETER	SYMBOLISM	RAINS SYMBOLISM
Amount of weathered silicate	WSi	-
Acid load	H	as
Base saturation	ß	ß
Cation exchange buffer capacity	ßCE	ßCE
Cation exchange capacity	CEC	CEC_{tot}
Conversion weathering rate to net surface lowering rate	f	-
Initial ßCE	ßCE0	-
Net surface lowering rate	NSLow	-
Silicate weathering rate within the cation exchange buffer range	brSi	br_{Si}
Silicate weathering rate within the $Al(OH)_3$ buffer range	$brSi_{Al}$	-
Silicate weathering rate constant	k_{si}	-
Soil formation rate	SoF	-
Total acidity	Htot	-

List of SKB reports

Annual Reports

1977-78
TR 121
KBS Technical Reports 1 – 120
Summaries
Stockholm, May 1979

1979
TR 79-28
The KBS Annual Report 1979
KBS Technical Reports 79-01 – 79-27
Summaries
Stockholm, March 1980

1980
TR 80-26
The KBS Annual Report 1980
KBS Technical Reports 80-01 – 80-25
Summaries
Stockholm, March 1981

1981
TR 81-17
The KBS Annual Report 1981
KBS Technical Reports 81-01 – 81-16
Summaries
Stockholm, April 1982

1982
TR 82-28
The KBS Annual Report 1982
KBS Technical Reports 82-01 – 82-27
Summaries
Stockholm, July 1983

1983
TR 83-77
The KBS Annual Report 1983
KBS Technical Reports 83-01 – 83-76
Summaries
Stockholm, June 1984

1984
TR 85-01
Annual Research and Development Report 1984
Including Summaries of Technical Reports Issued during 1984. (Technical Reports 84-01 – 84-19)
Stockholm, June 1985

1985
TR 85-20
Annual Research and Development Report 1985
Including Summaries of Technical Reports Issued during 1985. (Technical Reports 85-01 – 85-19)
Stockholm, May 1986

1986
TR 86-31
SKB Annual Report 1986
Including Summaries of Technical Reports Issued during 1986
Stockholm, May 1987

1987
TR 87-33
SKB Annual Report 1987
Including Summaries of Technical Reports Issued during 1987
Stockholm, May 1988

1988
TR 88-32
SKB Annual Report 1988
Including Summaries of Technical Reports Issued during 1988
Stockholm, May 1989

1989
TR 89-40
SKB Annual Report 1989
Including Summaries of Technical Reports Issued during 1989
Stockholm, May 1990

1990
TR 90-46
SKB Annual Report 1990
Including Summaries of Technical Reports Issued during 1990
Stockholm, May 1991

Technical Reports

List of SKB Technical Reports 1991

TR 91-01
Description of geological data in SKB's database GEOTAB
Version 2
Stefan Sehlstedt, Tomas Stark
SGAB, Luleå
January 1991

TR 91-02
Description of geophysical data in SKB database GEOTAB
Version 2
Stefan Sehlstedt
SGAB, Luleå
January 1991

TR 91-03
1. The application of PIE techniques to the study of the corrosion of spent oxide fuel in deep-rock ground waters
2. Spent fuel degradation
R S Forsyth
Studsvik Nuclear
January 1991

TR 91-04
Plutonium solubilities
I Puigdomènech[1], J Bruno[2]
[1]Enviromental Services, Studsvik Nuclear, Nyköping, Sweden
[2]MBT Tecnologia Ambiental, CENT, Cerdanyola, Spain
February 1991

TR 91-05
Description of tracer data in the SKB database GEOTAB
SGAB, Luleå
April, 1991

TR 91-06
Description of background data in the SKB database GEOTAB
Version 2
Ebbe Eriksson, Stefan Sehlstedt
SGAB, Luleå
March 1991

TR 91-07
Description of hydrogeological data in the SKB's database GEOTAB
Version 2
Margareta Gerlach[1], Bengt Gentzschein[2]
[1]SGAB, Luleå
[2]SGAB, Uppsala
April 1991

TR 91-08
Overview of geologic and geohydrologic conditions at the Finnsjön site and its surroundings
Kaj Ahlbom[1], Sven Tirén[2]
[1]Conterra AB
[2]Sveriges Geologiska AB
January 1991

TR 91-09
Long term sampling and measuring program. Joint report for 1987, 1988 and 1989. Within the project: Fallout studies in the Gideå and Finnsjö areas after the Chernobyl accident in 1986
Thomas Ittner
SGAB, Uppsala
December 1990

TR 91-10
Sealing of rock joints by induced calcite precipitation. A case study from Bergeforsen hydro power plant
Eva Hakami[1], Anders Ekstav[2], Ulf Qvarfort[2]
[1]Vattenfall HydroPower AB
[2]Golder Geosystem AB
January 1991

TR 91-11
Impact from the disturbed zone on nuclide migration – a radioactive waste repository study
Akke Bengtsson[1], Bertil Grundfelt[1],
Anders Markström[1], Anders Rasmuson[2]
[1]KEMAKTA Konsult AB
[2]Chalmers Institute of Technology
January 1991

TR 91-12
Numerical groundwater flow calculations at the Finnsjön site
Björn Lindbom, Anders Boghammar,
Hans Lindberg, Jan Bjelkås
KEMAKTA Consultants Co, Stockholm
February 1991

TR 91-13
Discrete fracture modelling of the Finnsjön rock mass
Phase 1 feasibility study
J E Geier, C-L Axelsson
Golder Geosystem AB, Uppsala
March 1991

TR 91-14
Channel widths
Kai Palmqvist, Marianne Lindström
BERGAB-Berggeologiska Undersökningar AB
February 1991

TR 91-15
Uraninite alteration in an oxidizing environment and its relevance to the disposal of spent nuclear fuel
Robert Finch, Rodney Ewing
Department of Geology, University of New Mexico
December 1990

TR 91-16
Porosity, sorption and diffusivity data compiled for the SKB 91 study
Fredrik Brandberg, Kristina Skagius
Kemakta Consultants Co, Stockholm
April 1991

TR 91-17
Seismically deformed sediments in the Lansjärv area, Northern Sweden
Robert Lagerbäck
May 1991

TR 91-18
Numerical inversion of Laplace transforms using integration and convergence acceleration
Sven-Åke Gustafson
Rogaland University, Stavanger, Norway
May 1991

TR 91-19
NEAR21 - A near field radionuclide migration code for use with the PROPER package
Sven Norman[1], Nils Kjellbert[2]
[1]Starprog AB
[2]SKB AB
April 1991

TR 91-20
Äspö Hard Rock Laboratory. Overview of the investigations 1986-1990
R Stanfors, M Erlström, I Markström
June 1991

TR 91-21
Äspö Hard Rock Laboratory. Field investigation methodology and instruments used in the pre-investigation phase, 1986-1990
K-E Almén, O Zellman
June 1991

TR 91-22
Äspö Hard Rock Laboratory. Evaluation and conceptual modelling based on the pre-investigations 1986-1990
P Wikberg, G Gustafson, I Rhén, R Stanfors
June 1991

TR 91-23
Äspö Hard Rock Laboratory. Predictions prior to excavation and the process of their validation
Gunnar Gustafson, Magnus Liedholm, Ingvar Rhén, Roy Stanfors, Peter Wikberg
June 1991

TR 91-24
Hydrogeological conditions in the Finnsjön area. Compilation of data and conceptual model
Jan-Erik Andersson, Rune Nordqvist, Göran Nyberg, John Smellie, Sven Tirén
February 1991

TR 91-25
The role of the disturbed rock zone in radioactive waste repository safety and performance assessment. A topical discussion and international overview.
Anders Winberg
June 1991

TR 91-26
Testing of parameter averaging techniques for far-field migration calculations using FARF31 with varying velocity.
Akke Bengtsson[1], Anders Boghammar[1], Bertil Grundfelt[1], Anders Rasmuson[2]
[1]KEMAKTA Consultants Co
[2]Chalmers Institute of Technology

TR 91-27
Verification of HYDRASTAR. A code for stochastic continuum simulation of groundwater flow
Sven Norman
Starprog AB
July 1991

TR 91-28
Radionuclide content in surface and groundwater transformed into breakthrough curves. A Chernobyl fallout study in an forested area in Northern Sweden
Thomas Ittner, Erik Gustafsson, Rune Nordqvist
SGAB, Uppsala
June 1991

TR 91-29
Soil map, area and volume calculations in Orrmyrberget catchment basin at Gideå, Northern Sweden
Thomas Ittner, P-T Tammela, Erik Gustafsson
SGAB, Uppsala
June 1991

TR 91-30
A resistance network model for radionuclide transport into the near field surrounding a repository for nuclear waste (SKB, Near Field Model 91)
Lennart Nilsson, Luis Moreno, Ivars Neretnieks, Leonardo Romero
Department of Chemical Engineering,
Royal Institute of Technology, Stockholm
June 1991

TR 91-31
Near field studies within the SKB 91 project
Hans Widén, Akke Bengtsson, Bertil Grundfelt
Kemakta Consultants AB, Stockholm
June 1991

TR 91-32
SKB/TVO Ice age scenario
Kaj Ahlbom[1], Timo Äikäs[2], Lars O. Ericsson[3]
[1]Conterra AB
[2]Teollisuuden Voima Oy (TVO)
[3]Svensk Kärnbränslehantering AB (SKB)
June 1991

TR 91-33
Transient nuclide release through the bentonite barrier - SKB 91
Akke Bengtsson, Hans Widén
Kemakta Konsult AB
May 1991

TR 91-34
SIMFUEL dissolution studies in granitic groundwater
I Casas[1], A Sandino[2], M S Caceci[1], J Bruno[1], K Ollila[3]
[1]MBT Tecnologia Ambiental, CENT, Cerdanyola, Spain
[2]KTH, Dpt. of Inorganic Chemistry, Stockholm, Sweden
[3]VTT, Tech. Res. Center of Finland, Espoo, Finland
September 1991

TR 91-35
Storage of nuclear waste in long boreholes
Håkan Sandstedt[1], Curt Wichmann[1], Roland Pusch[2], Lennart Börgesson[2], Bengt Lönnerberg[3]
[1]Tyréns
[2]Clay Technology AB
[3]ABB Atom
August 1991

TR 91-36
Tentative outline and siting of a repository for spent nuclear fuel at the Finnsjön site. SKB 91 reference concept
Lars Ageskog, Kjell Sjödin
VBB VIAK
September 1991

TR 91-37
Creep of OFHC and silver copper at simulated final repository canister-service conditions
Pertti Auerkari, Heikki Leinonen, Stefan Sandlin
VTT, Metals Laboratory, Finland
September 1991

TR 91-38
Production methods and costs of oxygen free copper canisters for nuclear waste disposal
Hannu Rajainmäki, Mikko Nieminen, Lenni Laakso
Outokumpu Poricopper Oy, Finland
June 1991

TR 91-39
The reducibility of sulphuric acid and sulphate in aqueous solution (translated from German)
Rolf Grauer
Paul Scherrer Institute, Switzerland
July 1990

TR 91-40
Interaction between geosphere and biosphere in lake sediments
Björn Sundblad, Ignasi Puigdomenech, Lena Mathiasson
December 1990

TR 91-41
Individual doses from radionuclides released to the Baltic coast
Ulla Bergström, Sture Nordlinder
Studsvik AB
May 1991

TR 91-42
Sensitivity analysis of the groundwater flow at the Finnsjön study site
Yung-Bing Bao, Roger Thunvik
Dept. Land and Water Resources,
Royal Institute of Technology, Stockholm, Sweden
September 1991

TR 91-43

SKB - PNC

Development of tunnel radar antennas

Lars Falk
ABEM, Uppsala, Sweden
July 1991

TR 91-44

Fluid and solute transport in a network of channels

Luis Moreno, Ivars Neretnieks
Department of Chemical Engineering,
Royal Institute of Technology, Stockholm, Sweden
September 1991